



Cite this: *Mater. Adv.*, 2024, 5, 3432

Unveiling the functional components and anti-Alzheimer's activity of *Koelreuteria elegans* (Seem.) A.C. Sm. using UHPLC-MS/MS and molecular networking[†]

Mohamed S. Demerdash,^{‡,a} Reem T. Attia,^{‡,b} Moshera M. El-Sherei,^a Wafaa M. Aziz,^a Sherif Ashraf Fahmy^{ID, *c} and Marwa Y. Issa^{ID, *a}

The use of plant extracts and their phytochemicals as candidates for treating Alzheimer's disease (AD) has been increasingly demanded lately. AD is a progressive neurodegenerative disorder, assumed to be associated with the formation of A β plaques and neurofibrillary tangles as well as with neuroinflammation, mediated by cytokines. The metabolomic profiles of *Koelreuteria elegans* (Seem.) A.C. Sm. leaf and fruit methanol extracts (KEL and KEF, respectively) were explored using UHPLC-MS/MS analysis aided by molecular networking in negative and positive modes for the first time. A total of 139 metabolites of different classes were tentatively identified. The molecular networking (MN) reflected high levels of phenolics and flavonoids. KEL and KEF showed great effects on memory function and spatial learning in behavioral experiments of the injured streptozotocin (STZ)-treated mice. The plant extracts led to pronounced improvement in the histopathological profile of the cerebral cortex of the injured STZ-treated mice. The effect of extracts on the levels of neuroinflammatory mediators TNF- α , NF- κ B and IL-1 β in AD-induced mice was assessed. Both extracts reduced all these markers of inflammation and neurodegeneration in AD.

Received 4th January 2024,
Accepted 25th February 2024

DOI: 10.1039/d4ma00007b

rsc.li/materials-advances

1. Introduction

Alzheimer's disease (AD) is the most common progressive neurodegenerative disorder, afflicting the health of the elderly. It primarily affects the hippocampal and cerebral cortex regions, causing deficits in memory, learning, thinking, and spatial orientation skills, as well as cognitive dysfunctions and personality alterations. The main pathological changes in the brain include the formation of extracellular senile plaques and neurofibrillary tangles and loss of neurons, leading to atrophy of the cerebral cortex, which is accompanied by a defect in the psychic and physical abilities.^{1,2} The chronic inflammatory processes accompanying AD played a key role in the development of

neurodegeneration in AD. Cytokines are products of the immune system and affect a wide range of biological functions, including immunity, inflammation and repair. Although most cytokines are produced at low levels in a healthy brain, neuroinflammation can be detected years before neuronal apoptosis. Pro-inflammatory cytokines represent immunoregulatory molecules that promote inflammation. The anti-inflammatory cytokines control the pro-inflammatory cytokine response. Inflammation is characterized by a co-ordination between pro- and anti-inflammatory cytokines and their imbalance may be an essential factor in AD.²

Tumor necrosis factor alpha (TNF- α), the most studied pro-inflammatory cytokine in the pathophysiology of AD, plays an important role in the cytokine cascade during an inflammatory response. The concentration of TNF- α increases in blood and the cerebrospinal fluid of AD patients as reported by many clinical and animal studies, indicating a link between the elevation of TNF- α levels in the brain and AD progression.³ Chronic neuronal TNF- α production causes synaptic dysfunction and severe neuronal death, leading to the evolution of AD and cognitive decline.⁴

Nuclear factor kappa B (NF- κ B) is an inflammatory transcription factor that fuels neurodegeneration. Upon exposure to pro-inflammatory mediators such as cytokines, NF- κ B target genes are activated and expressed, and consequent elevation of

^a Department of Pharmacognosy, Faculty of Pharmacy, Cairo University, Cairo 11562, Egypt. E-mail: marwa.issa@pharma.cu.edu.eg

^b Department of Pharmacology, Toxicology, and Biochemistry, Faculty of Pharmacy, Future University in Egypt, Cairo 11865, Egypt

^c Department of Chemistry, School of Life and Medical Sciences, University of Hertfordshire Hosted by Global Academic Foundation, R5 New Garden City, New Administrative Capital, AL109AB, Cairo 11835, Egypt.
E-mail: sheriffahmy@aucegypt.edu

[†] Electronic supplementary information (ESI) available. See DOI: <https://doi.org/10.1039/d4ma00007b>

[‡] Both authors contributed equally to this work.



cytokines and chemokines in microglia results in the chronic neuroinflammation observed in AD. Moreover, the elevation of NF- κ B levels in the cerebral cortex of AD patients is correlated with the formation of amyloid fibrils, which consequently aggregate into amyloid plaques.^{5,6}

Interleukin-1 (IL-1) is a pleiotropic cytokine family comprising a network of eleven pro-inflammatory cytokines capable of regulating acute and chronic inflammatory responses. Studies suggested the possible role of IL-1 in the immune processes in chronic neurodegenerative diseases, such as AD. The first members of the IL-1 family to be identified were IL-1 α and IL-1 β .² The pro-inflammatory cytokine IL-1 β has a critical modulatory effect in the pathogenesis of AD. Studies in human beings have demonstrated that an increase in IL-1 β expression has been associated with AD brain pathology. Experimental models showed that elevation of serum levels of IL-1 β is directly implicated in neurodegenerative injury and neural loss.^{7,8}

Koelreuteria elegans (Seem.) A.C. Sm. (*K. formosana* Hayata or *K. henryi* Dumm.) is a deciduous, ornamental landscape tree belonging to the family Sapindaceae, native to Taiwan and Fiji and also cultivated in South America, Australia and some Asian countries.⁹ It is a fast-growing species and tolerant of various environmental conditions.⁹ The plant species have been used in traditional Taiwanese medicine; its roots, bark, twigs, and leaves have been used to treat diarrhea, urethritis, and malaria and improve liver functions. Moreover the seeds of *K. elegans* were used as insecticides and the leaves as anti-fungal and anti-bacterial agents, besides being used as a black hair dye.¹⁰⁻¹⁵ Previous phytochemical studies of this species led to the identification of phenolic compounds, flavonoids, lignans, sterols, tocopherols and triterpenes.^{11,14-21} The metabolites of *K. elegans* form the basis for the determination of its biological activities. A great suppressive effect on dihydrodiol dehydrogenase expression has been demonstrated.²⁰ Protein-tyrosine kinase (PTK) was inhibited by kaempferol and quercetin and their glycosides that were isolated from the leaves and twigs;¹⁶ in addition, the antiproliferative activities of different fractions of isolated compounds against various human tumor cell lines were reported.^{11,14,17,22} Antioxidant and ROS scavenging activities of different fractions of leaf extract of *K. elegans*,^{21,23,24} aqueous extract of its flowers,¹³ and 1,3,4,5-tetra-O-galloylquinic acid isolated from the leaves¹⁹ and extracts of aerial plant parts¹² were documented. Furthermore, El Naggar demonstrated the antimicrobial activity of the aqueous methanolic extract of *K. elegans* leaves and its pure compounds, 1,3,4,5-tetra-O-galloylquinic acid butyl ester and methyl gallate, against *Geotrichum candidum*, *Staphylococcus aureus*, *Bacillus subtilis*, *Enterococcus faecalis*, *Salmonella typhimurium* and *Escherichia coli*, along with their hepatoprotective effect.¹⁵

Concerning current literature, nothing was found dealing with the identification and elucidation of the metabolite profiles of *K. elegans* leaf or fruit crude extracts or their anti-AD activity. This activity in genus *Koelreuteria* was only studied for *K. paniculata* Laxm.¹

Our study aimed to analyze the chemical profiles of *K. elegans* leaf and fruit methanol extracts by LC MS/MS-based

molecular networking in both negative and positive high-resolution electrospray ionization (ESI) modes to characterize their bioactive metabolites and find possible metabolomic differences. In addition, the effects of the tested samples on memory function and spatial learning in behavioral experiments and on the histopathological changes of the injured tissue induced by streptozotocin (STZ) in the cerebral cortex of the tested mice, as well as on the levels of elevated neuroinflammatory mediators TNF- α , NF- κ B and IL-1 β in the STZ-induced AD mouse model, were investigated.

2. Materials and methods

2.1. Plant materials

Fresh leaves and fruits of *Koelreuteria elegans* were collected in May 2021 from the Agriculture Research Centre, Giza, Egypt. The plant was kindly identified by Prof. Dr Abdel Halim Abdel Mojali, Head of the Department of Flora Researches and Plant Taxonomy at the Agriculture Research Centre, Giza, Egypt and was verified by Prof. Dr Rim Samir Hamdy, Professor of Plant Taxonomy and Flora at the Department of Botany, Faculty of Science, Cairo University. The plant materials were air-dried before being ground into a powder and kept in a closed container. A voucher specimen was deposited in the Herbarium of the Pharmacognosy Department at Cairo University under registration number 18.12.23.

2.2. Chemicals and reagents

For LC-MS/MS analysis, formic acid ($\geq 95.0\%$), water, acetonitrile, and methanol were of LC-MS grade and supplied by Merck (Darmstadt, Germany). The hematoxylin-eosin (H&E) staining kit (500 mL) was purchased from TissuePRO, catalogue #: 90888820. Thiopental sodium was obtained from EIPICO, 10th of Ramadan City, Egypt and formalin from the Gomhouria Company, Egypt, Catalogue #: L24810. TNF- α and IL-1 β ELISA kits were bought from CUSA-BIO Inc., Houston, TX, USA, Catalogue #: CSB-E11987r and the NF- κ B ELISA kit was purchased from EiAAB, Wuhan, China, Catalogue #: E1824r. All other solvents were of analytical grade.

2.3. Plant extraction

Four kilograms and 600 grams of air-dried powdered leaves and fruits, respectively, were separately extracted by cold maceration using methanol successively until exhaustion. Each extract was individually collected, evaporated to dryness at temperature not exceeding 40 °C under vacuum to obtain a dark green solid extract of leaves (KEL, 535 g) and a dark reddish solid extract of fruits (KEF, 40 g). The dried extracts were kept in a refrigerator at 4 °C for phytochemical and biological studies.

2.4. Sample preparation for UPLC-Orbitrap HRMS analysis

KEL and KEF, 100 mg each, were mixed with 5 mL of 100% MeOH containing 10 μ g mL⁻¹ umbelliferone as the internal standard, using a Turrax mixer (11 000 rpm) for five 20-s periods at 1 min intervals separating each period to prevent

heating. The extracts were vortexed vigorously and centrifuged at 3000 rpm for 30 min to remove debris and filtered using a 22 μm pore size filter. An aliquot of 500 μL was placed on a C18 cartridge (500 mg) preconditioned with MeOH and H₂O. Samples were then eluted with 5 mL of 100% MeOH, the eluent was evaporated under nitrogen stream, and the collected dry residue was resuspended in 500 μL of MeOH. Three microlitres of the supernatant were used for UPLC-MS analysis.

2.5. UPLC-Orbitrap HRMS analysis

Both negative and positive high-resolution ESI modes and collision-induced dissociation (CID) MS spectra were obtained using an Orbitrap Elite mass spectrometer (Thermo Fischer Scientific, Darmstadt, Germany) equipped with a heated electrospray ion source adjusted at 3 kV and 4 kV in negative and positive modes, respectively, with a capillary temperature of 300 °C, a source heater temperature of 250 °C, and an FTMS resolution of 30.000. The MS spectrometer was coupled to a UHPLC system (Dionex UltiMate 3000, Thermo Fischer Scientific), equipped with an RP-18 column (30 mm \times 2.1 mm \times 1.8 μm), Acquity HSS T3, H₂O, column temperature: 40 °C, DAD (220–600 nm, Thermo Fischer Scientific). The mobile phase consisted of H₂O (A) and acetonitrile (B) provided with 0.1% formic acid. The following elution gradient was used: at 0–1 min 5% (B), followed by linear increase to reach 100% B until 11 min, then from 11 to 19 min 100% (B) was used, and finally from 19 to 30 min (B) was reduced to 5%. The flow rate used was 150 $\mu\text{L min}^{-1}$ and the injection volume was 2 μL . The CID mass spectra were recorded using a normalized collision energy (NCE) of 35%. Calibration of the instrument was performed externally by using Pierce ESI negative ion calibration solution (Product no. 88324) and Pierce ESI positive ion calibration solution (Product no. 88323) from Thermo Fisher Scientific. The data were evaluated using Mass Hunter software version B.06.00.

2.6. LC-MS/MS data preparation

UPLC-MS files were converted into the mzXML format using the ProteoWizard tool MSConvert.²⁵ The converted data were processed using the free software MZmine 2.37 for peak picking, deconvolution, deisotoping, alignment, and formula prediction.

2.7. Feature-based molecular networking

The processed mzXML files were uploaded to the Global Natural Product Social Molecular Networking (GNPS) using the Winsep cross-platform. A feature-based molecular network (FBMN) in GNPS could integrate the spectral data to generate the molecular network, which compares and clusters the dataset. In the case of negative mode data, the setup parameters of the molecular network are as follows – network's basic options: precursor ion mass tolerance and fragment ion mass tolerance were set to 0.02 Da; advanced network options: minimum pairs cosine: 0.65; network TopK: 10; minimum matched fragment ions: 6; maximum connected component size: 100; maximum shift between precursors: 500 Da. All the other parameters were set to their default values. The same parameters processed the positive mode data; however, the minimum pairs cosine was set

to 0.55 and the minimum matched fragment ions were set to 3. The generated networks were imported to the open-source software platform, Cytoscape 3.10.0 software, for visualization.

2.8. Metabolites and molecular formula identification

The bioactive metabolites were identified in the extracts after processing UPLC-MS files using MZmine 2.37 software. The structural interpretation was achieved by extensively examining the high-resolution mass spectra. The CSI:FingerID interface of Sirius 5.6.3.0 software based on the high-resolution mass was used to identify or annotate the metabolites. Metabolite identification was further supported by MN exploration and the proposed GNPS spectral library search. The parameters of GNPS spectral library search were set to a precursor ion mass tolerance of 0.02 Da with minimum matched peaks of 4, a fragment ion mass tolerance of 0.02 Da and a score threshold of 0.65. According to the accurate mass and fragmentation pattern, the most likely molecular formula of the metabolite was selected and confirmed. PubChem, HMDB, Reaxys, LIPID MAPS and COCONUT were also used.

2.9. Neuroprotective activity of KEL and KEF

2.9.1. Animals. Male albino mice ($n = 24$) weighing 25–30 g were purchased from the National Research Institute in Egypt. Animals were housed in an air-conditioned room under controlled alternate day and night cycles provided with artificial fluorescent light. They were fed a standard pellet diet and water *ad libitum*. These conditions were evaluated on a daily basis to ensure the safety and well-being of the animals. A veterinarian checked the health of animals to ensure the lack of clinically observable abnormalities.

The study was approved and all methods were performed in agreement with the appropriate guidelines and protocols of the Ethics Committee for Animal Experimentation of Faculty of Pharmacy, Cairo University (Permit Number: MP 3324) and conform to the Guide for the Care and Use of Laboratory Animals published by the US National Institutes of Health (NIH Publication No. 85-23, revised 2011).

2.9.2. Acute toxicity test. The oral acute toxicity study of KEL and KEF was carried out using the 'Up-and-Down' method²⁶ of testing on mice at single-graded doses of 175 to 2000 mg kg⁻¹ body weight and up to 5000 mg kg⁻¹ body weight in accordance with the Organization for Economic Development (OECD) guideline no. 425.²⁷ Five male mice were used for each dose level in the study. An animal was picked at a time, weighed and dosed with the equivalent volume of extract dissolved in distilled water. Animals were kept fasting overnight (about 18 h) before administering the doses. Then, the extract was administered orally using a gastric feeding tube. Each animal was observed after dosing for the first 5 min for signs of regurgitation and kept in a metallic cage. Each animal was then observed every 15 min in the first 4 h, then every 30 min for 6 h, and daily for 48 h for behavioral signs of toxicity according to the specifications of the OECD.²⁷ The animals were monitored for a total of 14 days for the long-term possible lethal outcome.



2.9.3. Experimental model for neuroprotective activity. In this research, Alzheimer's disease was induced through the intracerebroventricular (ICV) injection of streptozotocin (STZ), utilizing the freehand technique originally outlined^{28,29} but with modifications as illustrated.³⁰ STZ was administered at a dosage of 3 mg kg^{-1} , dissolved in 0.9% sterile saline solution. To anesthetize the mice, xylazine (10 mg kg^{-1} , i.p.) and ketamine (80 mg kg^{-1} , i.p.) were employed. In brief, the head was stabilized by applying downward pressure just above the ears, and the lateral ventricle was identified by forming an equilateral triangle between the eyes and the centre of the skull to locate the bregma. The needle was inserted through the skin and skull approximately 1 mm lateral to this reference point. Within one minute of STZ administration, the mice exhibited normal behavior. The animals were randomly divided into four groups, each consisting of six mice. Group 1, referred to as the normal control group (NC), animals received a single ICV injection of $3 \mu\text{L}$ 0.9% sterile saline solution. In contrast, groups 2, 3, and 4 received a single ICV injection of STZ (3 mg kg^{-1}) dissolved in $3 \mu\text{L}$ 0.9% sterile saline.³¹ Group 2 served as the positive control (PC), while groups 3 and 4 received treatment with KEL and KEF (300 mg kg^{-1} orally), respectively, for 60 days. The extracts were administered to the mice *via* gastric gavage, and equivalent volumes of saline were given to the NC and PC groups.

The Morris water maze (MWM; probe test) and object recognition tests were performed 24 h following the last administration of either extract. In order to reduce variability resulting from circadian rhythms, the tests were consistently conducted at approximately the same time each day. Following the behavioral assessments, each group was further divided into two subgroups (with $n = 3$ in each), and the mice were euthanized using an overdose injection of thiopental (IP 200 mg kg^{-1}). The brains were rapidly extracted and separated. One set of whole brains were preserved in 10% formalin in saline for subsequent histopathological and immunohistochemical examination, while the brains of the other set were designated for biochemical analyses.

2.9.4. Morris water maze. The swimming maze used in the experiment was a large circular pool measuring 150 cm in diameter and 60 cm in height. The pool was filled with water up to a depth of 30 cm and maintained at room temperature. Notably, four specific points on the tank's rim were labeled as north (N), south (S), east (E), and west (W), effectively dividing the pool into four quadrants (NW, NE, SE, and SW). This division was achieved by attaching two threads perpendicular to each other on the pool rim. Within one of these quadrants, a submerged platform measuring 10 cm in width and 28 cm in height, painted black, was consistently positioned just 2 cm below the water surface. The water was made opaque to make the platform invisible by adding a harmless dye (powdered non-fat milk). During the training, control mice quickly learned to swim directly toward the hidden platform, reaching it in a short time. This training was conducted over four consecutive days. Each mouse underwent two consecutive trials on the first three days, with a minimum 15-minute gap between them. If a mouse

managed to locate the concealed platform within the allotted 120 seconds, it was allowed to stay there for an additional 20 seconds before being removed. However, if it failed to find the hidden platform within the specified time, it was gently guided to it and allowed to stay for 20 seconds. The average time taken by each mouse to find the hidden platform during the four-day training phase was defined as the mean escape latency (MEL). This measurement was recorded for each mouse during every trial conducted.³² On the fifth day, a probe test was carried out for all groups to locate the hidden platform, and each mouse was given 60 seconds to explore the pool. The time spent by each mouse in the target quadrant, where the previously hidden platform was located, was then calculated.

2.9.5. Tissue extract. Animals were sacrificed using a lethal dose of thiopental (IP 200 mg kg^{-1}), and each group was further divided into two subgroups (with $n = 3$ in each). The brains were rapidly extracted and separated. One set of whole brains were preserved in 10% formalin in saline for subsequent histopathological and immunohistochemical examination, while the brains of the other set were kept at -80°C and homogenized before biochemical analyses.

2.9.6. Histopathological examination. The brains of three representative rats from each experimental group were carefully removed and then immersed in a 10% formalin saline solution for a 24-hour fixation period. Afterward, they were rinsed with tap water and subjected to treatment with a series of alcohol solutions for gradual dehydration. The brain specimens were then made transparent using xylene and embedded in paraffin, which was melted at 56°C in a hot air oven for another 24 hours. Paraffin blocks containing the brain samples were sliced into thin sections, approximately $4 \mu\text{m}$ thick, using a sledge microtome. These resulting tissue sections were placed on glass slides and any remaining paraffin was removed. Finally, the sections were stained with hematoxylin and eosin (H&E) for subsequent examination under a light microscope.

3. Results

3.1. LC-MS/MS metabolomic profiling aided by molecular networking

Metabolomic profiling conducted using UHPLC-MS/MS analysis aided by MN in negative and positive modes was performed to assess the metabolite composition of *K. elegans* leaf and fruit extracts. The analysis led to the characterization of several known compounds that were detected before in the *Koelreuteria* genus or discovered for the first time. Metabolomic assessments were made by comparing retention times, distribution, accurate masses and fragmentation patterns, which were further supported by MN exploration, together with the proposed GNPS spectral library search, followed by literature data comparison for confirmation. The metabolites along with their peak numbers, observed m/z of the detected molecular ions, errors (ppm), molecular formulae, product ions (MS/MS), compound classes, and retention times are presented in Table 1. The representative base peak chromatograms of the



Table 1 Compounds identified in *K. elegans* leaf and fruit methanol extracts by LC-MS/MS in negative and positive ESI modes

Peak RT	Assignment	Precursor ion (<i>m/z</i>)	Error (ppm)	Molecular formula	Product ions MS/MS	Class	KEL KEF
1	0.90 Theogallin isomer I	343.0656[M - H] ⁻	-2.62	C ₁₄ H ₁₆ O ₁₀	191, 169, 125	Phenolic acid	+
2	0.90 Methyl- <i>O</i> -galloyl hexoside isomer I	345.0812[M - H] ⁻	-2.90	C ₁₄ H ₁₈ O ₁₀	345, 169, 124, 151, 161, 191, 85	Phenolic acid	+
3	0.90 Quinic acid	191.0553[M - H] ⁻	-1.57	C ₇ H ₁₂ O ₆	85, 191, 59, 93, 127, 109, 111, 173	Organic acid	+
4	0.92 Di- <i>O</i> -galloylquinic acid isomer I	495.0757[M - H] ⁻	-3.64	C ₂₁ H ₂₀ O ₁₄	169, 343, 325, 495	Phenolic acid	+
5	0.93 Gallic acid	169.0136[M - H] ⁻	-0.59	C ₇ H ₆ O ₅	125, 79, 69, 81, 97, 107, 53	Phenolic acid	-
6	0.94 Tri- <i>O</i> -galloylquinic acid isomer I	647.0862[M - H] ⁻	-3.34	C ₂₈ H ₂₄ O ₁₈	495, 647, 343, 477, 325, 169, 191	Phenolic acid	+
7	0.95 Proline betaine	144.1017[M + H] ⁺	-5.55	C ₇ H ₁₃ NO ₂	144, 58, 84, 102	Amino acid betaine	+
8	0.95 Methyl- <i>O</i> -galloyl hexoside isomer I	347.0963[M + H] ⁺	-4.32	C ₁₄ H ₁₈ O ₁₀	153, 109, 125, 347, 81, 155, 145	Phenolic acid	+
9	0.97 Tetra- <i>O</i> -galloylquinic acid isomer I	799.0965[M - H] ⁻	-3.63	C ₃₆ H ₂₈ O ₂₂	601, 629, 477, 169, 647, 495, 343, 191	Phenolic acid	+
10	0.98 Digallic acid isomer I	321.0238[M - H] ⁻	-2.80	C ₁₄ H ₁₀ O ₉	169, 125	Phenolic acid	+
11	1.13 Betaine	118.0860[M + H] ⁺	-6.77	C ₅ H ₁₁ NO ₂	59, 58, 118	Modified amino acid	+
12	1.31 Shikimic acid	173.0448[M - H] ⁻	-1.16	C ₇ H ₁₀ O ₅	93, 73, 83, 137	Organic acid	+
13	1.43 Guanidinobutanoic acid	146.0920[M + H] ⁺	-6.16	C ₁₃ H ₁₁ NO ₂	87, 86, 60, 69, 83, 146, 56, 111	Organic acid	+
14	1.59 Galloyl hexoside isomer I	331.0656[M - H] ⁻	-2.72	C ₁₃ H ₁₆ O ₁₀	169, 331, 151, 211, 125, 271, 89	Phenolic acid	+
15	1.63 Theogallin isomer I	345.0811[M + H] ⁺	-3.19	C ₁₄ H ₁₆ O ₁₀	153, 125, 79, 81, 171, 229, 85	Phenolic acid	+
16	1.73 Theogallin isomer II	343.0656[M - H] ⁻	-2.62	C ₁₄ H ₁₆ O ₁₀	169, 191, 125	Phenolic acid	-
17	2.03 Isoleucine	132.1017[M + H] ⁺	-6.06	C ₆ H ₁₃ NO ₂	86, 69, 58, 57, 91	Amino acid	+
18	2.70 Galloyl hexoside isomer II	331.0656[M - H] ⁻	-2.72	C ₁₃ H ₁₆ O ₁₀	169, 331, 151, 59, 123, 211, 271, 89	Phenolic acid	+
19	2.86 Pyrogallol	127.0387[M + H] ⁺	-6.30	C ₆ H ₆ O ₃	81, 53, 109, 79, 67	Phenol	-
20	2.89 Gallic acid	171.0285[M + H] ⁺	-5.26	C ₇ H ₆ O ₅	81, 107, 109, 125, 153, 53, 79, 69, 97	Phenolic acid	+
21	2.94 Pyrogallol	125.0239[M - H] ⁻	0	C ₆ H ₆ O ₃	125, 79, 51, 97, 81, 107	Phenol	+
22	3.38 Galloyl hexoside isomer III	331.0656[M - H] ⁻	-2.72	C ₁₃ H ₁₆ O ₁₀	169, 214, 271, 125, 331, 59, 89, 151	Phenolic acid	+
23	3.72 Methyl- <i>O</i> -galloyl hexoside isomer II	347.0966[M + H] ⁺	-3.46	C ₁₄ H ₁₈ O ₁₀	153, 127, 109, 349, 125, 155, 81, 174	Phenolic acid	+
24	3.80 Methyl- <i>O</i> -galloyl hexoside isomer III	345.0811[M - H] ⁻	-3.19	C ₁₄ H ₁₈ O ₁₀	345, 169, 124, 151, 193, 161	Phenolic acid	+
25	3.97 Proto catechic acid isomer I	153.0187[M - H] ⁻	-0.65	C ₇ H ₆ O ₄	109, 81, 53	Phenolic acid	+
26	4.10 Theogallin isomer II	345.0812[M + H] ⁺	-2.90	C ₁₄ H ₁₆ O ₁₀	153, 174, 111, 125, 51, 327, 109	Phenolic acid	+
27	4.67 Phenylalanine	166.0861[M + H] ⁺	-4.21	C ₉ H ₁₁ NO ₂	120, 103, 84, 93, 77, 91	Amino acid	+
28	4.75 Galloyl hexoside isomer IV	331.0656[M - H] ⁻	-2.72	C ₁₃ H ₁₆ O ₁₀	271, 169, 211, 125, 59, 151	Phenolic acid	+
29	5.31 Proto catechic acid hexoside isomer I	315.0708[M - H] ⁻	-2.54	C ₁₃ H ₁₆ O ₉	153, 109, 108, 152	Phenolic acid	+
30	5.35 Methyl- <i>O</i> -galloyl hexoside isomer III	347.0967[M + H] ⁺	-3.17	C ₁₄ H ₁₈ O ₁₀	153, 109, 127, 79, 81, 171, 53, 329, 141	Phenolic acid	+
31	5.44 Methyl- <i>O</i> -galloyl hexoside isomer III	345.0812[M - H] ⁻	-2.90	C ₁₄ H ₁₈ O ₁₀	345, 124, 169, 151, 161, 85	Phenolic acid	+
32	5.97 Theogallin isomer III	343.0655[M - H] ⁻	-2.91	C ₁₄ H ₁₆ O ₁₀	191, 169, 125	Phenolic acid	+
33	6.13 Theogallin isomer III	345.0813[M + H] ⁺	-2.61	C ₁₄ H ₁₆ O ₁₀	153, 125, 345, 171, 285, 107, 285	Phenolic acid	+
34	6.15 Proto catechic acid hexoside isomer II	153.0187[M - H] ⁻	-0.65	C ₇ H ₆ O ₄	109, 81, 53, 91	Phenolic acid	+
35	6.65 Proto catechic acid hexoside isomer II	315.0706[M - H] ⁻	-3.17	C ₁₃ H ₁₆ O ₉	152, 108, 153, 315, 109	Phenolic acid	+
36	7.75 Galloylglycerol	243.0498[M - H] ⁻	-4.90	C ₁₀ H ₁₂ O ₇	153, 125, 107, 140, 79	Phenolic acid	+
37	7.79 Galloylglycerol	243.0498[M - H] ⁻	-2.88	C ₁₀ H ₁₂ O ₇	124, 169, 243, 59, 151, 89, 91	Phenolic acid	+
38	7.81 Galloyl di-hexoside	493.1176[M - H] ⁻	-3.65	C ₁₉ H ₂₆ O ₁₅	493, 313, 169, 271, 191, 331, 125	Phenolic acid	+
39	7.93 Methyl gallate hexoside	345.0811[M - H] ⁻	-3.19	C ₁₄ H ₁₈ O ₁₀	183, 59, 225, 89, 285, 71, 169, 124	Phenolic acid	+
40	7.97 Salicylic acid hexoside	299.0759[M - H] ⁻	-2.67	C ₁₃ H ₁₆ O ₈	137, 59, 89, 101, 93, 119	Phenolic acid	+
41	8.07 Galloylshikimic acid isomer I	325.0550[M - H] ⁻	-3.08	C ₁₄ H ₁₄ O ₉	169, 125, 325, 173, 93, 111	Phenolic acid	+
42	8.17 Galloylshikimic acid isomer II	327.0706[M + H] ⁺	-3.06	C ₁₄ H ₁₄ O ₉	153, 95, 109, 125, 171, 139, 214	Phenolic acid	+
43	8.41 Syringic acid hexoside	383.0945[M + Na ⁺]	-2.35	C ₁₅ H ₂₀ O ₁₀	383, 224, 185, 251, 253	Phenolic acid	+
44	8.47 Hydroxybenzoic acid	137.0239[M - H]/139.0387[M + H] ⁺	-0/3.5	C ₇ H ₆ O ₃	93, 137, 108, 119/77, 124, 95, 65, 56	Phenolic acid	+
45	8.56 Hydroxyquinoline	146.0598[M + H] ⁺	-5.48	C ₉ H ₇ NO	146, 7, 91, 118, 104, 128	Hydroquinolone	+
46	8.66 Tri- <i>O</i> -galloylquinic acid isomer II	647.0861[M - H] ⁻	-3.55	C ₂₈ H ₂₄ O ₁₈	477, 647, 495, 343, 169, 449, 325, 191	Phenolic acid	+
47	8.67 Methyl gallate hexoside	359.0967[M + H] ⁺	-3.06	C ₁₅ H ₁₈ O ₁₀	153, 111, 93, 171, 127, 359, 143, 167	Phenolic acid	+
48	8.69 Tri- <i>O</i> -galloylshikimic acid	631.0925[M + H] ⁺	-1.58	C ₂₈ H ₂₂ O ₁₇	153, 461, 631	Phenolic acid	-
49	8.70 Di- <i>O</i> -galloylshikimic acid isomer I	479.0815[M + H] ⁺	-2.30	C ₂₁ H ₁₈ O ₁₃	153, 309, 479, 171, 95	Phenolic acid	-
50	8.72 Di- <i>O</i> -galloylquinic acid isomer II	495.0758[M - H] ⁻	-3.43	C ₂₁ H ₂₀ O ₁₄	343, 169, 495, 325, 191	Phenolic acid	+

Table 1 (continued)

Peak RT	Assignment	Precursor ion (<i>m/z</i>)	Error (ppm)	Molecular formula	Product ions MS/MS	Class	KEL KEF
51 8.76	Methyl gallate	183.0293[M - H] ⁻	-0.55	C ₈ H ₈ O ₃	124, 183, 78, 168	Phenolic acid	- +
52 8.81	Galloylshikimic acid isomer II	327.0706[M + H] ⁺	-3.06	C ₁₄ H ₁₄ O ₉	153, 95, 139, 143, 255, 279, 111	Phenolic acid	+ +
53 8.81	Di-O-galloylquinic acid	497.0920[M + H] ⁺	-2.21	C ₂₁ H ₂₀ O ₁₄	153, 309, 327, 479, 328, 171, 125	Phenolic acid	+ +
54 8.83	Kynurenic acid	190.0496[M + H] ⁺	-4.21	C ₁₀ H ₁₂ NO ₃	144, 116, 113, 89, 162, 59	Organic acid	+ +
55 8.88	Methyl gallate	185.0443[M + H] ⁺	-3.78	C ₈ H ₈ O ₅	126, 153, 107, 125, 59, 67, 95, 79	Phenolic acid	+ +
56 8.99	Digallic acid	323.0394[M + H] ⁺	-2.79	C ₁₄ H ₁₀ O ₉	153, 125, 79	Phenolic acid	+ +
57 9	Catechin/Epicatechin	289.0707[M - H] ⁻	-1.73\ -3.78	C ₁₅ H ₁₄ O ₆	247, 109, 203, 191, 123, 219, 179, 151\139,	Flavonoid	+ +
58 9.02	Digallic acid isomer II	291.0858[M + H] ⁺	-2.49	C ₁₄ H ₁₀ O ₉	123, 147, 207, 140, 177, 162	Phenolic acid	+ +
59 9.13	Scopoletin isomer I	321.0239[M - H] ⁻	-5.18	C ₁₄ H ₁₀ O ₉	169, 125	Phenolic acid	+ +
60 9.14	Brevifolin carboxylic acid	193.0491[M + H] ⁺	-5.18	C ₁₀ H ₈ O ₄	133, 178, 193, 137, 105, 194, 122, 109, 80,	Hydroxycoumarin	+ +
61 9.21	Trimethoxyphenol	291.0134[M - H] ⁻	-2.41\ -3.07	C ₁₃ H ₈ O ₈	247, 191, 219, 147, 229/219, 191, 247, 293,	Isocoumarin	+ +
62 9.30	Di-O-galloylshikimic acid isomer II	293.0288[M + H] ⁺	-2.41\ -3.07	C ₁₃ H ₈ O ₈	149, 76	Isocoumarin	+ +
63 9.30	Tri-O-galloylquinic acid isomer III	185.0805[M + H] ⁺	-4.86	C ₉ H ₁₂ O ₄	120, 205, 163, 179	Phenol	+ +
64 9.41	Tetra-O-galloylquinic acid isomer II	479.0816[M + H] ⁺	-2.09	C ₂₂ H ₁₈ O ₁₃	125, 153, 110, 139, 127, 59, 95, 107, 79	Phenolic acid	+ -
65 9.44	Tetra-O-galloylapiptiitol isomer I	647.0863[M - H] ⁻	-3.25\ -2.16	C ₂₈ H ₂₄ O ₁₈	153, 309, 479, 171, 95	Phenolic acid	+ +
66 9.53	3-Methoxy-4-hydroxyphenol-1-O- β -d-(6'-O-galloyl)-glucoside isomer I	649.1027[M + H] ⁺	-3.50	C ₃₅ H ₂₈ O ₂₂	495, 647, 343, 477, 325, 169, 191/153, 479,	Phenolic acid	+ +
67 9.62	Kaempferol rutinoside isomer I	799.0966[M - H] ⁻	-1.02	C ₃₃ H ₂₈ O ₂₁	305, 263, 309, 631, 461, 281, 171	Phenolic acid	+ +
68 9.77	Galloyl-(<i>epi</i>)-galloocatechin (epi)galloocatechin	783.1029[M + Na] ⁺	2.84	C ₂₀ H ₂₂ O ₁₃	799, 601, 629, 477, 169, 647, 495, 343, 191	Phenolic acid	+ +
69 9.81	Calcosin hexoside	493.097[M + Na] ⁺	-1.68	C ₂ H ₃₀ O ₁₅	C ₃₃ H ₃₀ O ₁₈	Phenolic acid	+ +
70 9.84	Tetra-O-galloylapiptiitol isomer II	447.1280[M + H] ⁺	7.99	C ₂ H ₃₀ O ₁₅	287, 449, 71, 85, 243, 147, 153	Flavonoid	+ +
71 9.98	Cirsimarin hexoside	783.1026[M + Na] ⁺	-2.46	C ₂₂ H ₂₂ O ₁₀	C ₃ H ₃₀ O ₁₈	Flavonoid	+ +
72 10.05	Vanilin	477.1385[M + H] ⁺	0.63	C ₃₃ H ₂₈ O ₂₁	285, 153, 447, 309, 270	Flavonoid	- -
73 10.08	Quercetin di-deoxyhexoside	153.0544[M + H] ⁺	-2.51	C ₂₃ H ₂₄ O ₁₁	C ₃ H ₃₀ O ₁₈	Flavonoid	+ +
74 10.13	Quercetin rutinoside	593.1485[M - H] ⁻	-4.57	C ₈ H ₈ O ₃	315, 475, 153	Flavonoid	+ +
		609.1433[M - H] ⁻	-3.71	C ₂ H ₃₀ O ₁₅	65, 93, 110, 125, 79	Flavonoid	+ +
		611.1600[M + H] ⁺	-3.76/ -2.37	C ₂₇ H ₃₀ O ₁₆	593, 447, 284, 301, 183, 299, 271	Flavonoid	- -
		633.1417[M - 2.00\ -2.37]			609, 300, 301/303, 85, 129, 71, 465/633, 331, Flavonoid	Flavonoid	+ +
75	10.20 3-Methoxy-4-hydroxyphenol-1-O- β -D-(6'-O-galloyl)-glucoside isomer II	493.097[M + Na] ⁺	2.43	C ₂₀ H ₂₂ O ₁₃	325, 153	Flavonoid	+ +
76	10.20 1'-O-galloyl-3,4,5-trihydroxybenzyl alcohol	645.1078[M + Na] ⁺	1.55	C ₂₂ H ₂₆ O ₁₇	153, 475, 645, 305, 323, 273	Phenolic acid	+ +
77	10.26 Ellagic acid	300.9977[M - H] ⁻	-2.33\ -2.64	C ₁₄ H ₆ O ₈	301/303, 285, 275, 165, 237, 137, 153	Phenolic acid	+ +
78	10.26 Quercetin hexoside	303.0132[M + H] ⁺	-3.24/	C ₂₁ H ₂₀ O ₁₂	300, 463, 271, 178, 151, 255/303, 91, 85, 61, Flavonoid	Phenolic acid	+ +
		463.0862[M - H] ⁻	-2.58\ -2.67	C ₉ H ₁₀ O ₅	305, 97, 73, 127/487, 185, 325	Flavonoid	+ +
		465.1021[M + H] ⁺			95	Flavonoid	+ +
79	10.27 Kaempferol rutinoside	593.1484[M - H] ⁻	-3.88	C ₂ H ₃₀ O ₁₅	593, 285	Phenolic acid	+ +
80	10.28 Catechin gallate	441.0807[M - H] ⁻	-3.40	C ₂₂ H ₁₈ O ₁₀	169, 289, 245, 125	Flavonoid	+ +
81	10.32 Kaempferol hexoside	449.1073[M + H] ⁺	-2.45	C ₂ H ₃₀ O ₁₁	287	Flavonoid	+ +
82	10.37 Syringic acid	197.0447[M - H] ⁻	-1.52\ -4.02	C ₉ H ₁₀ O ₅	123, 182, 97, 167/140, 107, 167, 59, 123, 67, Phenolic acid	Flavonoid	+ +
83	10.45 Scopoletin isomer II	193.0492[M + H] ⁺	-4.66	C ₁₀ H ₈ O ₄	178, 133, 193, 137, 149, 122, 194, 105, 165	Hydroxycoumarin	+ +
84	10.45 Kaempferol rutinoside isomer II	595.1650[M + H] ⁺	-2.18	C ₂ H ₃₀ O ₁₅	150, 111, 94	Flavonoid	+ +
85	10.54 Kaempferol hexoside	471.0893[M + Na] ⁺	-2.12	C ₂₁ H ₂₀ O ₁₁	287, 85, 71, 129, 449	Flavonoid	+ +



Table 1 (continued)

Peak RT	Assignment	Precursor ion (<i>m/z</i>)	Error (ppm)	Molecular formula	Product ions MS/MS	Class	KEL KEF
86	10.55 Quercetin pentoside	433.0757[M - H] ⁻ /435.0918[M + H] ⁺ /457.0736[M + Na] ⁺	-3.23/-2.07/-2.41	C ₂₀ H ₁₈ O ₁₁	300, 433, 271, 178, 151/303, 73, 305, 61, 115/ Flavonoid	+	+
87	10.65 Methyl digallate	335.0395[M - H] ⁻ /337.0550[M + H] ⁺	-2.39/-3.00	C ₁₅ H ₁₂ O ₉	183, 124, 168, 78/153, 125, 185	Phenolic acid	+
88	10.66 Diosmetin	303.0703[M + H] ⁺	-3.00	C ₁₆ H ₁₂ O ₆	301, 286, 258, 153	Flavonoid	+
89	10.70 Quercetin isomer I	303.0496[M + H] ⁺	-3.00	C ₁₅ H ₁₀ O ₇	303, 153, 229, 285, 165	Flavonoid	+
90	10.75 Isorhamnetin hexoside	501.0995[M + Na] ⁺	-2.79	C ₂₂ H ₂₂ O ₁₂	501, 339, 185, 317	Flavonoid	+
91	10.76 Apigenin hexoside isomer I	433.1123[M + H] ⁺	-2.77	C ₂₁ H ₂₀ O ₁₀	271	Flavonoid	-
92	10.85 Kaempferol pentoside	417.0809[M - H] ⁻ /441.0792[M + Na] ⁺	-3.12/-1.36	C ₂₀ H ₁₈ O ₁₀	284, 417, 255, 227, 151/441, 309, 155	Flavonoid	+
93	10.90 Diosmetin hexoside	463.1231[M + H] ⁺	-1.94	C ₂₂ H ₂₂ O ₁₁	301, 286, 258	Flavonoid	+
94	10.92 Kaempferide hexoside	461.1069[M - H] ⁻	-3.25	C ₂₂ H ₂₂ O ₁₁	461, 283, 298, 255, 269, 315	Flavonoid	+
95	10.96 Phloretin	275.0911[M + H] ⁺	-3.27	C ₁₅ H ₁₄ O ₅	107, 169, 77	Dihydrochalcone	+
96	10.99 Phloretin hexoside isomer I	435.1275[M - H] ⁻	-3.68	C ₂₁ H ₂₄ O ₁₀	273, 167, 341, 391, 125	Dihydrochalcone	+
97	11.12 Kaempferol isomer I	287.0545[M + H] ⁺	-3.83	C ₁₅ H ₁₀ O ₆	287, 153, 121, 165	Flavonoid	+
98	11.12 Apigenin hexoside isomer II	433.1124[M + H] ⁺	-2.54	C ₂₁ H ₂₀ O ₁₀	271	Flavonoid	+
99	11.13 Kaempferol deoxyhexoside	431.0964[M - H] ⁻ /455.0943[M + Na] ⁺	-3.25/-2.42	C ₂₁ H ₂₀ O ₁₀	285, 431, 255, 227/309, 455, 169, 310, 85, 71	Flavonoid	+
100	11.28 Phloretin hexoside isomer II	435.1272[M - H] ⁻ /599.1016[M + H] ⁺	-4.37	C ₂₁ H ₂₄ O ₁₀	273, 167, 221, 191, 315	Dihydrochalcone	+
101	11.45 Quercetin galloyl deoxyhexoside	601.1180[M + H] ⁺ /623.0999[M + Na] ⁺	-3.51/-2.16/-2.25	C ₂₈ H ₂₄ O ₁₅	599, 304, 297, 169/153, 299, 154, 303, 300/ Flavonoid	+	
102	11.54 Dihydrokaempferol	287.0549[M - H] ⁻	-2.44	C ₁₅ H ₁₂ O ₆	135, 123, 151, 183, 223	Flavonoid	+
103	11.80 Daidzein hexoside	417.1174[M + H] ⁺	-2.64	C ₂₁ H ₂₀ O ₉	255	Flavonoid	+
104	11.85 Luteolin	287.0545[M + H] ⁺	-3.83	C ₁₅ H ₁₀ O ₆	287, 197, 257, 152, 269	Flavonoid	-
105	11.87 Quercetin isomer II	303.0495[M + H] ⁺	-3.30	C ₁₅ H ₁₀ O ₇	303, 285, 165, 257, 229, 153	Flavonoid	+
106	11.87 Kaempferol galloyl deoxyhexoside	583.1065[M - H] ⁻ /607.1048[M + Na] ⁺	-3.94/-2.64	C ₂₈ H ₂₄ O ₁₄	285, 583, 297, 169/321, 607, 303, 281, 153, 175	Flavonoid	+
107	11.89 Quercetin	301.0340[M - H] ⁻	-2.66	C ₁₅ H ₁₀ O ₇	151, 301, 179, 121, 107, 65	Flavonoid	+
108	11.94 Isorhamnetin	315.0497[M - H] ⁻	-2.54	C ₁₆ H ₁₂ O ₇	300, 125, 315, 112, 187, 71	Flavonoid	-
109	12.52 Isosakuranetin rutinoside	593.1847[M - H] ⁻	-3.88	C ₂₈ H ₃₄ O ₁₄	285	Flavonoid	+
110	12.57 Undecanedioic acid	215.1279[M - H] ⁻	-1.86	C ₁₁ H ₂₀ O ₄	197, 153, 215	Fatty acid	+
111	12.62 Trihydroxyacetecadienoic acid	327.2162[M - H] ⁻	-3.06	C ₁₈ H ₃₂ O ₅	327, 211, 229, 171, 85, 97, 291	Fatty acid	+
112	12.66 Kaempferol isomer II	285.0391[M - H] ⁻ /287.0547[M + H] ⁺	-2.81/-3.14	C ₁₅ H ₁₀ O ₆	285/287, 153, 121, 165	Flavonoid	+
113	12.76 Diosmetin	299.0546[M - H] ⁻	-3.34	C ₁₆ H ₂₀ O ₆	284, 299, 256, 79	Flavonoid	+
114	13.02 Trihydroxyacetecenoic acid	329.2319[M - H] ⁻	-2.73	C ₁₈ H ₃₄ O ₅	329, 211, 171, 229, 139, 99	Fatty acid	+
115	13.30 Dodecanedioic acid	229.1435[M - H] ⁻	-2.18	C ₁₂ H ₂₂ O ₄	211, 167, 229	Fatty acid	+
116	14.22 Chrysin	253.0495[M - H] ⁺	-2.37	C ₁₅ H ₁₀ O ₄	253, 158, 177, 209, 63, 143, 79	Flavonoid	+
117	15.39 DGMG (18: 3)	721.3616[M + HCOO] ⁻	-4.30	C ₃₁ H ₅₆ O ₁₄	397, 675, 415, 277, 235, 721, 253	Glycolipid	+
118	15.76 Sideroxylin	311.0909[M - H] ⁻	-3.54	C ₁₈ H ₁₆ O ₅	296, 311	Flavonoid	+
119	15.94 PI (18: 2/0: 0)	595.2859[M - H] ⁻	-4.03	C ₂₇ H ₄₉ O ₁₂ P	595, 279, 153, 315, 241, 415, 79, 259	Phosphoinositol	+
120	16.04 DGMG (18: 2)	723.3772[M + HCOO] ⁻	-4.29	C ₃₃ H ₅₈ O ₁₄	397, 677, 415, 279, 89, 235, 305, 723, 253	Glycolipid	+
121	16.14 PC (18: 3/0: 0)	518.3232[M + H] ⁺	-2.89	C ₂₆ H ₄₈ NO ₇ P	184, 104, 518, 300, 86, 258, 60, 125	Phosphocholine	-
122	16.23 DGMG (16: 0) isomer I	699.3773[M + HCOO] ⁻	-4.29	C ₃₁ H ₅₈ O ₁₄	397, 653, 415, 255, 235, 699, 89, 253	Glycolipid	+
123	16.38 PE (18: 2/0: 0)	476.2759[M - H] ⁻	-3.78	C ₂₃ H ₄₄ NO ₇ P	279, 476, 196, 214, 79, 140, 153	Phosphoethanolamine	+
124	16.42 MGMG 18: 3	559.3097[M + HCOO] ⁻	-3.75	C ₂₇ H ₄₆ O ₉	277, 103, 513	Glycolipid	+
125	16.46 PI (16: 0)	571.2863[M - H] ⁻	-3.50	C ₂₅ H ₄₉ O ₁₂ P	571, 255, 153, 241, 315, 393, 79, 259	Phosphoinositol	+
126	16.52 DGMG (16: 0) isomer II	699.3776[M + HCOO] ⁻	-3.86	C ₃₁ H ₅₈ O ₁₄	397, 653, 415, 255, 235, 89, 699, 253	Glycolipid	+
127	16.66 PE (16: 0/0: 0) isomer I	452.2760[M - H] ⁻	-3.76	C ₂₁ H ₄₄ NO ₇ P	255, 113, 452, 181, 153, 79, 214, 140	Phosphoethanolamine	-
128	16.96 PE (16: 0/0: 0) isomer II	452.2759[M - H] ⁻	-3.98	C ₂₁ H ₄₄ NO ₇ P	255, 452, 196, 140, 79, 214, 153	Phosphoethanolamine	+



Table 1 (continued)

Peak RT	Assignment	Precursor ion (<i>m/z</i>)	Error (ppm)	Molecular formula	Product ions MS/MS	Class	KEL KEF
129	17.07 PC (18:2)	520.3391[M + H] ⁺	-2.31	C ₂₀ H ₃₀ NO ₂ P	104, 520, 502, 86, 337, 60, 258	Phosphocholine	+
130	17.19 Linoleic acid	561.3253[M - H] ⁻	-3.92	C ₂₈ H ₅₀ O ₁₁	279, 253, 504, 235	Fatty acid	+
131	17.41 PA (18:2/0:0)	433.2339[M - H] ⁻	-3.69	C ₂₁ H ₃₉ O ₇ P	153, 79, 433, 171, 97, 279	Phosphatidic acid	+
132	17.78 Palmitic-oleic acid	537.3253[M - H] ⁻	-4.09	C ₂₆ H ₅₀ O ₁₁	255, 253, 235	Fatty acid	+
133	18.03 PC (16:0)	496.3389[M + H] ⁺	-2.82	C ₂₄ H ₅₀ NO ₂ P	104, 184, 496, 478, 86, 258, 313	Phosphocholine	+
134	18.20 PA (0:0/16:0)	409.2341[M - H] ⁻	-3.42	C ₁₉ H ₃₉ O ₇ P	153, 79, 409, 255, 97	Phosphatidic acid	+
135	18.67 PA (18:1/0:0)	435.2495[M - H] ⁻	-3.91	C ₂₁ H ₄₁ O ₇ P	153, 79, 97, 171, 281	Phosphatidic acid	+
136	20.3 Hydroxyicosanoic acid isomer I	327.2887[M - H] ⁻	-3.67	C ₂₀ H ₄₀ O ₃	59, 255, 101, 327	Fatty acid	+
137	20.30 PA (18:3/16:0) isomer I	669.4466[M - H] ⁻	-4.33	C ₃₇ H ₇₇ O ₈ P	391, 669, 255, 409, 153, 79, 277, 413, 97	Phosphatidic acid	+
138	20.88 Hydroxyicosanoic acid isomer II	327.2889[M - H] ⁻	-3.06	C ₂₀ H ₄₀ O ₃	59, 327, 101	Fatty acid	-
139	23.33 PA (18:3/16:0) isomer II	669.4467[M - H] ⁻	-4.18	C ₃₇ H ₆₇ O ₈ P	391, 669, 255, 79, 153, 409, 413, 277, 97	Phosphatidic acid	+

Note: DGMG, digalactosyldimonoacylglycerol; MGGM, monogalactosyldimonoacylglycerol; PE, phosphoethanolamine; PC, phosphocholine; PA, phosphatidic acid and PI, phosphoinositol.

two extracts along with detailed fragmentation labelling of some identified compounds are displayed in Fig. 1 and Fig. S1–S21 (ESI[†]). Putative structures of representative groups of metabolites are shown in Fig. 2. A total of 139 metabolites were identified after overlapping both negative and positive data of KEL and KEF. The chief identified secondary metabolites were phenolics and flavonoids (a total of ninety-four), as confirmed by previous reports.^{14–16,18,20–22} Negative and positive MNs were established (Fig. 3 and 4). They allowed us to investigate UPLC-MS/MS data and observe metabolite distribution among the two samples in both modes. Depending on MS/MS fragmentation pattern similarities, they classified molecules into clusters, where metabolites with fragmentation patterns close enough to each other were connected, while those with dissimilar fragmentation patterns were separated,³³ based on controlled parameters described before. Nodes were displayed as a pie chart to describe the semi-relative abundance of the detected molecular ions in the two extracts, while the edges indicated the mass differences between the connected nodes. Nodes were also colored by the sample type (*i.e.*, KEL and KEF) and labeled with their precursor *m/z* values. The established MN of the negative mode was composed of 590 nodes connected in twenty-six clusters (a minimum of two connected nodes) and 350 self-looped nodes. The detected metabolites are identified as follows: phenolic acids: clusters A, B, and C; flavonoids: cluster D; cluster E was mostly formed by the assigned lipids; glycolipids were arranged in cluster F; most of the determined fatty acids were present in clusters G, H, and I; two phosphatidic acids were formed in cluster J; and cluster K comprised one dihydrochalcone. Regarding self-looped nodes, they mostly corresponded to some flavonoids and phenolic acids, among other metabolites. The constructed MN of positive mode consisted of 833 nodes comprising thirty-six clusters (a minimum of two connected nodes) and 561 self-looped nodes. Cluster A' encompassed phenolic acids, while clusters B', C', D' and E' represented flavonoids. Phosphocholines were arranged in cluster F'. The identified hydroxyquinoline occurred in cluster H' and cluster G' contained amino acids, organic acids, phenols, hydroxycoumarins and an isocoumarin. Some flavonoids and phenolic acids besides a dihydrochalcone were arranged in single-looped nodes.

3.1.1. Phenolic acids and derivatives. The term “phenolic acids” generally describes the phenolic compounds having one carboxylic acid group.³⁴ Numerous phenolic acids and their conjugates have been previously reported in *K. elegans* along with their antioxidant, anti-inflammatory,^{12,13,19,21,23} anti-cancer,^{14,22} antimicrobial and hepatoprotective effects.¹⁵ In this study, fifty-seven phenolic acids were tentatively identified, and they are mainly derivatives of hydroxybenzoic acids present as esters, glycosides, or glycoside-esters. Herein, the main phenolic components were gallic, syringic and protocatechuic acids, which were found mainly conjugated with quinic or shikimic acids or glycosides with one or more sugar units. Phenolic acids and their derivatives constituted clusters A, B, C (in the negative mode MN) and A' (in the positive mode MN) alongside single nodes in both modes. Galloyl derivatives were considered the

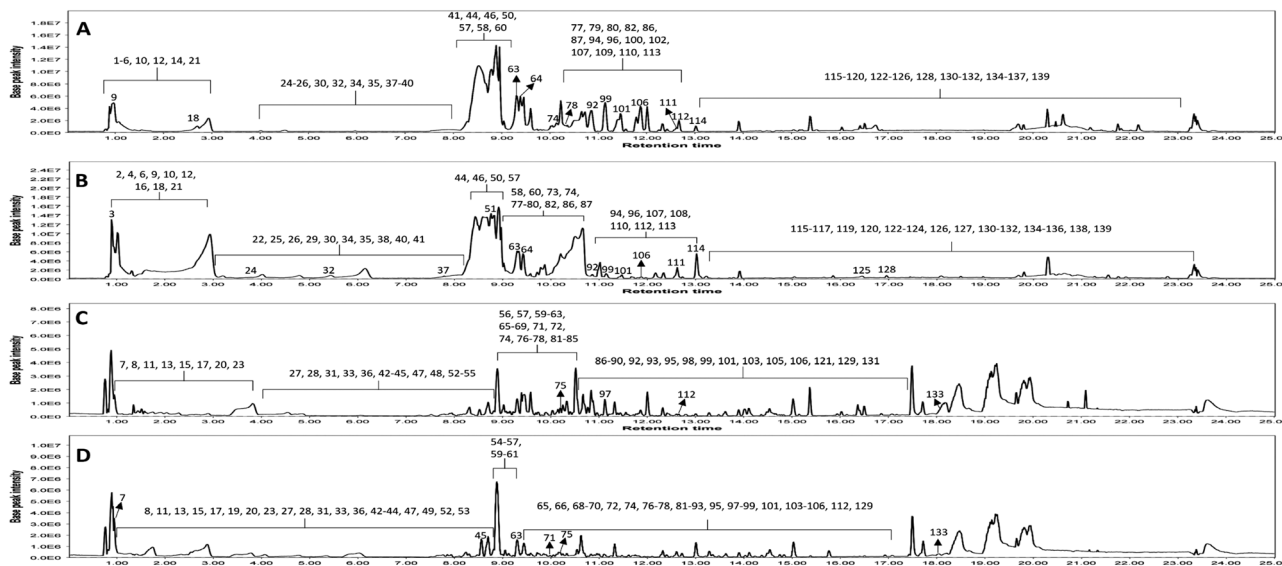


Fig. 1 LC-MS base peak chromatograms of KEL and KEF in negative and positive ESI modes. (A) negative KEL; (B) negative KEF; (C) positive KEL and (D) positive KEF. KEL, *Koelreuteria elegans* leaf extract and KEF, *Koelreuteria elegans* fruit extract.

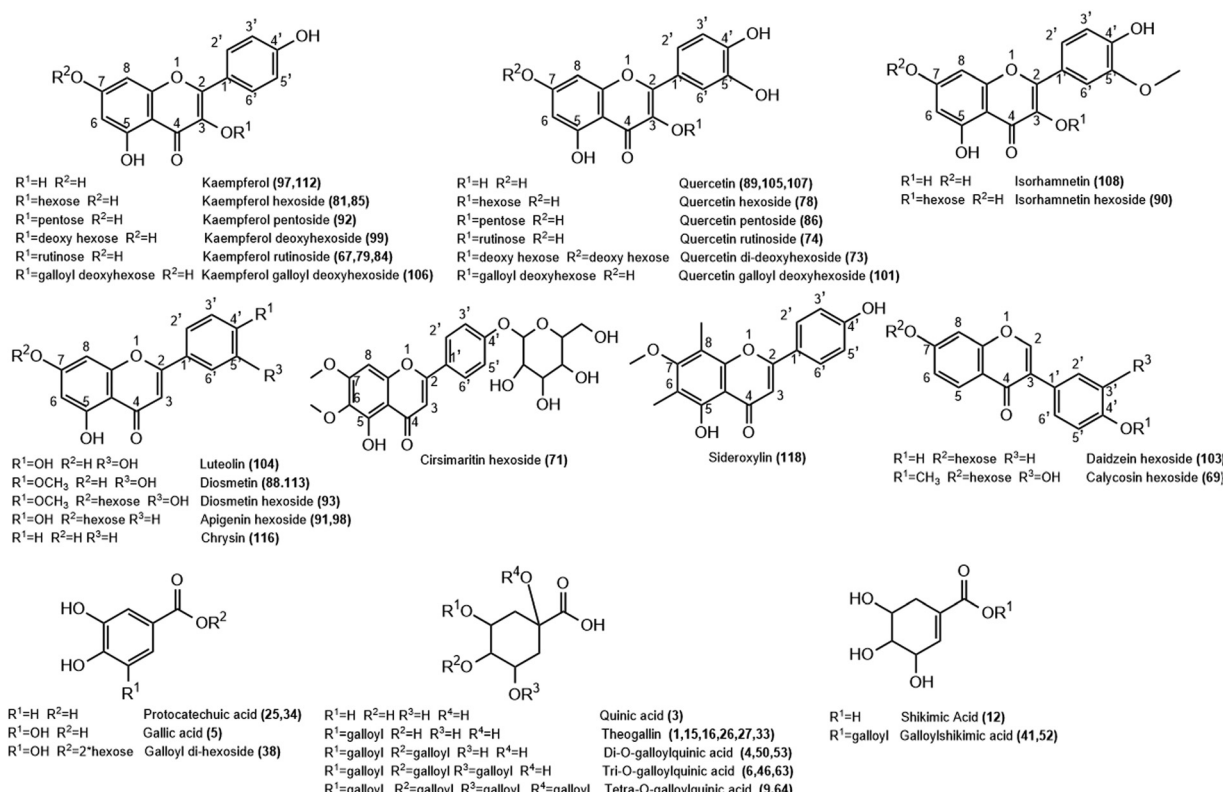


Fig. 2 Structure of representative groups of metabolites identified in the *K. elegans* leaf methanol extract (KEL) and *K. elegans* fruit methanol extract (KEF). The carbon numbering system for each compound is based on analogy rather than on IUPAC rules. Metabolite numbers are listed in Table 1.

major phenolic acid compounds and showed higher abundance in KEF than in KEL, as highlighted mainly in the MN. Cluster A revealed the presence of nineteen galloyl esters displaying a fragment ion at m/z 169 due to the liberation of

gallate ions. Galloyl quinic acid molecules were detected as peaks 1, 6, 9, 16, 32, 46, 50, 63 and 64. These compounds were composed of quinic acid as the central unit, attached with the gallate ion or its multiples. Their fragmentation behavior



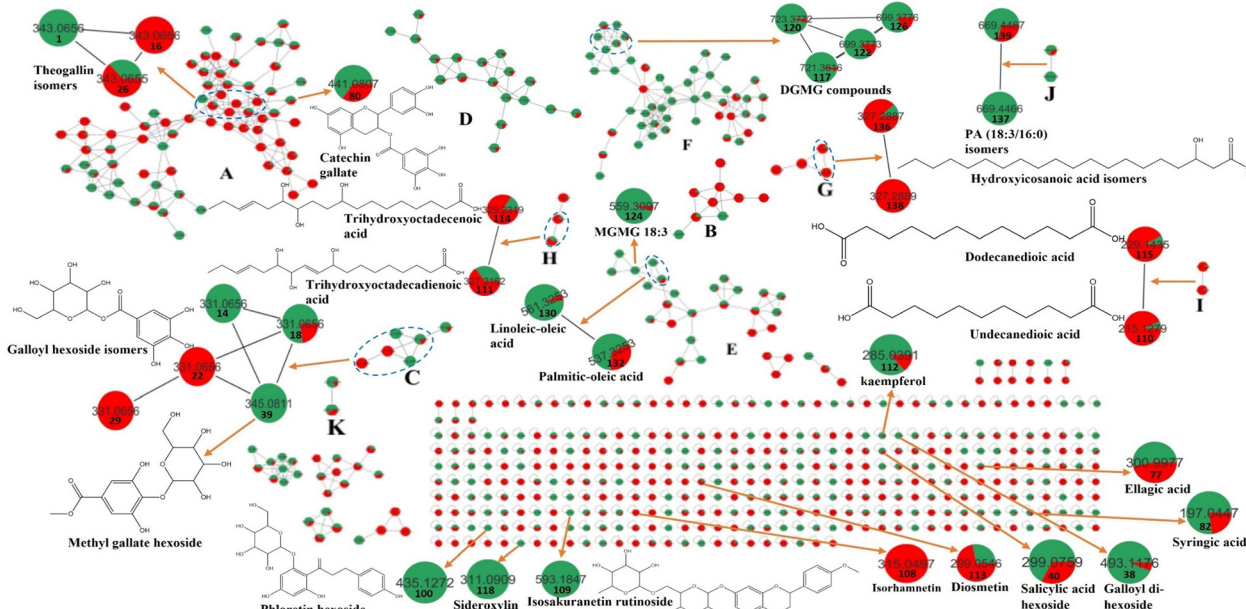


Fig. 3 Molecular network established using MS/MS data in the negative ESI mode from the LC-MS/MS analysis of *K. elegans* leaf and fruit extracts. The pie charts reflect the relative abundance of the detected molecular ions. Selected nodes and clusters have been zoomed-in. KEL (green color): *Koelreuteria elegans* leaf methanol extract, KEE (red color): *Koelreuteria elegans* fruit methanol extract.

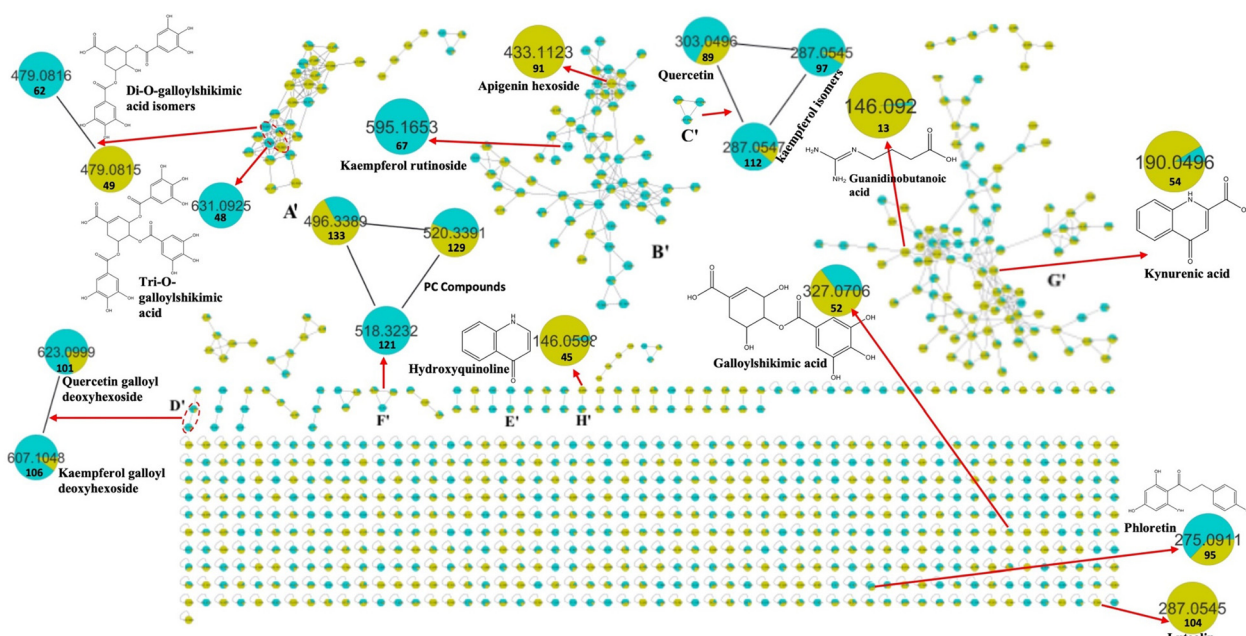


Fig. 4 Molecular network established using MS/MS data in the positive ESI mode from the LC-MS/MS analysis of *K. elegans* leaf and fruit extracts. The pie charts reflect the relative abundance of the detected molecular ions. Selected nodes and clusters have been zoomed-in. KEL (turquoise color): *Koelreuteria elegans* leaf methanol extract. KEF (olive green color): *Koelreuteria elegans* fruit methanol extract.

depended mainly on successive loss of the dehydrated gallate anion (-152 amu) until the appearance of the quinic acid peak (m/z 19). Quinic acid attached to one gallate unit in peaks **1**, **16** and **32** showed nearly similar molecular ion masses and fragmentation patterns and they were considered as 3 isomers

of the same compound identified as theogallin; isomer **1** was observed in KEL only, while **16** was observed in KEF; isomer **32** was present in both and was more abundant in fruits than in leaves. Peak **50** revealed $[M - H]^-$ at *m/z* 495.0758 related to an extra gallate anion. It was identified as di-*O*-galloylquinic acid.

Tri-*O*-galloylquinic acid was detected at 3 different retention times of 0.94, 8.66 and 9.30 min (peaks **6**, **46** and **63**) with $[M - H]^-$ at *m/z* at 647.0862, 647.0861 and 647.0863, respectively; they had similar fragment ions. Four gallic acid units conjugated with quinic acid were observed at peaks **9** and **64** with $[M - H]^-$ at *m/z* 799.0965 and 799.0966, respectively. Their similar product ions revealed that they were two isomers, putatively identified as tetra-*O*-galloylquinic acid. Two isomers of digallic acid were observed; peaks **10** and **58** with $[M - H]^-$ at *m/z* 321.0238 and 321.0239, respectively, fragmented into *m/z* 169 and 125 corresponding to the galloyl ion and loss of CO_2^- , respectively. Peak **37** was assigned as galloylglycerol with fragment ions *m/z* 169, 124 and 91 due to gallic acid, decarboxylation, and glycerol, respectively. Peak **41** showed $[M - H]^-$ at *m/z* 325.0550, putatively named galloylshikimic acid. It exhibited fragment ions at *m/z* 169, 125, 173, 111 and 93 due to gallate ions, loss of CO_2^- , shikimic ions, further decarboxylation, and dehydration, respectively. Galloyl methyl esters were detected as peaks **51** and **87** annotated as methyl gallate (*m/z* 183.0293) and methyl digallate (*m/z* 335.0395), respectively. Both showed product ions related to the loss of CH_3 (−15 Da) and CO_2 (−44) groups. Furthermore, compound **87** revealed a fragment ion at *m/z* 183 due to loss of a galloyl moiety (−152 Da). Four hydroxybenzoic acids (**5**, **25**, **34** and **44**) were present in cluster B. Compound **5** was identified as gallic acid, compounds **25** and **34** were considered as two isomers of protocatechuic acid detected at different *t_r* and compound **44** was hydroxybenzoic acid. These compounds showed a base peak at *m/z* 125, 109 and 93, respectively, due to decarboxylation and other fragment ions mainly due to further dehydration. Peaks **14**, **18**, **22** and **29** in cluster C revealed the same $[M - H]^-$ at *m/z* 331.0656 and showed the typical fragmentation pattern of hexoside as evident from the loss of the fragment ion $[M - 162]^-$ at *m/z* 169. Therefore, those compounds were isomers of galloyl hexoside, but isomer **14** was present in KEL, **22** and **29** were present in KEF and isomer **18** was more abundant in leaves than in fruits. Compound **39** at the same cluster showed *m/z* at 345.0811 with a mass difference of 14 Da and an extra ion at 183 *m/z*, indicative of an extra methyl esterification, and was identified as methyl gallate hexoside. Cluster A' represented peaks of phenolic acids, which were subjected to positive mode analysis. Twenty-two peaks (**8**, **15**, **23**, **26**, **30**, **33**, **36**, **42**, **47**, **48**, **49**, **53**, **56**, **62**, **63**, **65**, **66**, **68**, **70**, **75**, **76** and **87**) and their possible neutral losses in the MS/MS analysis were putatively identified, corresponding to the galloyl moiety, with most of them being displayed in negative mode interpretation. Inspection of their MS² spectra displayed base peaks at *m/z* 153 corresponding to dehydroxylated galloyl fragment ions. Compounds **8**, **23** and **30** with $[M + H]^+$ at *m/z* 347.0963, 347.0966 and 347.0967, respectively, were determined as 3 isomers of methyl-*O*-galloyl hexoside due to their fragmentation similarity and equalization of their molecular ion mass. Galloyl quinic (peaks **15**, **26**, **33**, **47**, **53** and **63**) and galloyl shikimic (peaks **42**, **48**, **49** and **62**) containing molecules represented most of the remaining compounds. Moreover, theogallin was eluted at 3 different *t_r* of 1.63, 4.10 and 6.13 min (peaks **15**, **26** and **33**, respectively) and with

$[M + H]^+$ at *m/z* 345.0811, 345.0812 and 345.0813, respectively. Compounds **47**, **53** and **63**, with $[M + H]^+$ at *m/z* 359.0967, 497.0920 and 649.1027, respectively, were assigned as methyl galloylquinic acid, di-*O*-galloylquinic acid and tri-*O*-galloylquinic acid, respectively. Peak **42** was characterized as galloylshikimic acid (*m/z* at 327.0706), peak **48** was identified as tri-*O*-galloylshikimic acid (*m/z* at 631.0925), detected in KEL only, and peaks **49** and **62** were identified as 2 isomers of di-*O*-galloylshikimic acid with $[M + H]^+$ at *m/z* 479.0815 and 479.0816, respectively; isomer **49** was identified in fruits, while the other was identified in leaves. Finally, peaks **38**, **40**, **77** and **82** were scattered in self-looped nodes of the negative MN. Compound **38** was identified with $[M - H]^-$ at *m/z* 493.1176 as galloyl di-hexoside due to loss of the di-hexoside unit (−324 Da) at 169 *m/z* and the remaining ions belonged to sugar fragmentation as determined previously.³⁵ Compounds **40** and **82** were identified as salicylic acid hexoside and syringic acid with $[M - H]^-$ at *m/z* 299.0759 and 197.0447, respectively. Compound **40** revealed product ions at *m/z* 137, 119, and 93 corresponding to salicylic acid, dehydration, and decarboxylation, respectively, while peak **82** showed fragment ions at *m/z* 182, 167 and 123 due to loss of a methyl group, further loss of a methyl group, and loss of one CO_2 , respectively. Ellagic acid was present as peak **77** with $[M - H]^-$ at *m/z* 300.9977. It had a sharp molecular ion peak (*m/z* 301) in agreement with a reported article.³⁶

3.1.2. Flavonoids. Flavonoids are an important class of natural products; particularly, they belong to a class of plant secondary metabolites having a polyphenolic structure.³⁷ They have biochemical and antioxidant effects associated with various diseases, such as cancer, and they have been previously reported in the *Koelreuteria* genus.^{16,20,35} Thirty-seven flavonoids of different classes were tentatively identified with their possible product ions by the MS/MS analysis. They comprised mainly cluster D in the negative MN and clusters B', C', D', and E' in the positive MN and a few of them were detected in other clusters and single nodes. The examined flavonoids were flavonols (kaempferol, quercetin and isorhamnetin), flavones (apigenin, luteolin, diosmetin, chrysanthemum, sideroxylin and cirsimarin), isoflavones (calycosin), flavanols (catechin or epicatechin) and only one flavanone (isosakuranetin) aglycone.

3.1.2.1. Flavonols. Twenty-two flavonols were detected in *K. elegans* methanolic extracts, including 12 kaempferols: two of them were isomers of kaempferol aglycone (peaks **97** and **112**), one as dihydrokaempferol (peak **102**) and nine as glycosides (peaks **67**, **79**, **81**, **84**, **85**, **92**, **94**, **99** and **106**), 8 quercetin isomers; 3 of them as aglycones (peaks **89**, **105** and **107**) and 5 as glycosides (peaks **73**, **74**, **78**, **86** and **101**) and 2 isorhamnetin isomers (peaks **90** and **108**). Furthermore, peaks **67** and **102** were observed only in KEL, while peaks **73** and **108** were noticed only in KEF. Indeed, most of the displayed flavonols were represented by *O*-glycosides that showed a higher abundant ion $[Aglycone - H]^-/[Aglycone + H]^+$, derived from a homolytic cleavage, at *m/z* 285/287 (kaempferol), and 301/303 (quercetin) relative to the corresponding ion $[Aglycone]^-$, derived from a



heterolytic cleavage, at m/z 284 and 300, respectively. Specifically, rutinosyl glycosides were observed in compounds **74** and **79**, which showed $[M - H]^-$ at m/z 609.1433 and 593.1484, respectively. After losing the rutinosyl moiety, the fragments ions **301** and **285** were produced, indicating quercetin and kaempferol aglycones, respectively. Aglycone hexosides were detected as peaks **78**, **85** and **90** with $[M + Na]^+$ at m/z 487.084, 471.0893 and 501.0995, respectively. They revealed the $[A g l y c o n e + N a]^+$ ion peaks at m/z 325 (quercetin), **309** (kaempferol) and **339** (isorhamnetin), respectively, after loss of the hexose moiety. Compounds **86** (m/z 433.0757) and **92** (m/z 417.0809) revealed aglycone product ions at m/z 300 and 284, respectively due to loss of the pentose sugar unit. Compounds **73** and **99** (m/z 593.1485 and 431.0964, respectively) were identified as quercetin di-deoxyhexoside and kaempferol deoxy hexoside based on the relative abundances of the aglycone ion after the loss of di-deoxy (−292 Da) and deoxy (−146 Da) hexose moieties, respectively. Peak **94** was putatively identified as kaempferide hexoside with m/z 461.1069 $[M - H]^-$. It exhibited product ions at m/z 446 and 283 due to successive loss of methyl and hexose moieties, in addition to the fragment ion at m/z 298 due to direct loss of the hexose unit from the parent mass corresponding to kaempferide aglycone. Methyl ether of quercetin or isorhamnetin (peak **108**) showed a molecular ion peak at m/z 315.0497 and a fragment ion peak at 300 m/z due to loss of the methyl group (−15 Da). Finally, compounds **101** and **106** showed conjugation between sugar and galloyl moieties. They were annotated as quercetin galloyl deoxy hexoside (m/z 599.1016) and kaempferol galloyl deoxy hexoside (m/z 583.1065), respectively. They showed fragment ions at m/z 169 and 297 corresponding to galloyl and dehydrated galloyl deoxy hexose moieties, respectively.

3.1.2.2. Flavones and isoflavones. Nine flavones (peaks **71**, **88**, **91**, **93**, **98**, **104**, **113**, **116** and **118**) were tentatively detected in both leaf and fruit extracts. However, peaks **91** and **104** could not be identified in KEL, while peak **118** was absent in KEF. They were present as aglycones aside from peaks **71**, **91**, **93** and **98**, which were present in the form of glycosides. Compound **71** showed m/z 477.1385 $[M + H]^+$ and was identified as cirsimarin hexoside. It had a base peak at m/z 315 due to loss of the hexose unit. Similarly, peaks **91** and **98** revealed an aglycone abundant fragment ion at 271 m/z belonging to apigenin after losing the sugar moiety. Their $[M + H]^+$ species were nearly similar: m/z 433.1123 and 433.1124, respectively, and they were considered as isomers of apigenin hexoside. Luteolin-containing compounds are listed in Table 1 as peaks **88**, **93**, **104** and **113** based on the relative abundances of the aglycone ion. Compound **104** showed m/z 287.0545 $[M + H]^+$ corresponding to luteolin aglycone. Compounds **88** and **113** were tentatively identified as diosmetin, while **93** was their glycosidic form (m/z 463.1231 $[M + H]^+$) due to loss of hexose sugar (m/z 301 m/z). Diosmetin produced product ions at m/z 286 and 284 due to loss of the methyl group (−15 Da) in positive (peaks **88** and **93**) and negative (peak **113**) analyses, respectively. Peak **116** was identified as chrysin with $[M - H]^-$ at m/z 253.0495. Peak

118 was identified as sideroxylin (311.0909 m/z) with a fragment ion at m/z 296 due to demethylation. Isoflavones were represented as peaks **69** (m/z 447.1280) and **103** (m/z 417.1174), which were identified as calycosin and daidzein hexosides, respectively. They showed $[A g l y c o n e + H]^+$ product ions at m/z 285 and 255, respectively, due to loss of sugar unit. Furthermore, peak **69** revealed a fragment ion at m/z 270 corresponding to demethylation of calycosin aglycone.

3.1.2.3. Flavanols and flavanones. Flavan-3-ols or catechins were detected as peaks **57**, **68** and **80** and are listed in Table 1. They were tentatively characterized as catechin/epicatechin, galloyl-(*epi*)-gallocatechin-(*epi*)-gallocatechin and catechin gallate, respectively. Compound **57** revealed m/z at 289.0707 $[M - H]^-$ and 291.0858 $[M + H]^+$, while **68** showed $[M + K]^+$ at m/z 801.1133. Their fragmentation patterns were in agreement with the reported literature.³⁸ Peak **80** showed a conjugation between galloyl and catechin units with fragment ions at m/z 289 and 169 due to loss of galloyl ions and gallic acid, respectively. Finally, only one flavanone was observed in KEL and was identified as isosakuranetin rutinoside, peak **109**. It revealed m/z 593.1847 $[M - H]^-$ with abundant $[A g l y c o n e - H]^-$ at m/z 285 due to loss of the rutinosyl moiety.

It is worth noting that the established MN was capable of discriminating ions from several flavonoid analogues as observed for the negative MN. Cluster D was considered the main cluster for flavonoid glycosides. Catechin gallate was separated from the main flavonoid cluster and presented in cluster A. This might be due to the presence of galloyl moiety, which was the main part of cluster A. Sideroxylin, isorhamnetin, diosmetin, and kaempferol aglycones appeared as self-looped nodes, due to the absence of sugar moieties. In the positive MN, cluster B' included flavonoid glycosides, cluster C' contained aglycones only and D' included galloyl flavonol glycosides.

3.1.3. Fatty acids and lipids. MS/MS analysis revealed several fatty acids, *e.g.*, peaks **110**, **111**, **114**, **115**, **130**, **132**, **136** and **138**, which were mainly unsaturated and/or hydroxylated. They appeared in the negative MN as clusters E, F, G, H, and I. The main fragmentation of fatty acids included the loss of water and carbon dioxide molecules from the parent molecular ion.³⁹ Cluster E had two of the fatty acids as peaks **130** and **132** with $[M - H]^-$ at m/z 561.3253 and 537.3253, respectively. Due to their molecular ion masses and fragmentation patterns, which agreed with the previous literature,⁴⁰ compounds **130** and **132** were annotated as linoleic-oleic and palmitic-oleic acids, respectively. Two isomers of hydroxyicosanoic acid were detected in cluster G with m/z at 327.2887 and 327.2889 and listed as peaks **136** and **138**, respectively. Isomer **138** was present in fruits only. Cluster H contained two of the identified fatty acids at peaks **111** [m/z 327.2162 ($C_{18}H_{31}O_5^-$)] and **114** [m/z 329.2319 ($C_{18}H_{33}O_5^-$)] with a mass difference of 2 amu, indicative of an extra double bond in **111**, and were identified as trihydroxyoctadecadienoic and trihydroxyoctadecenoic acids, respectively. Peaks **110** [m/z 215.1279 ($C_{11}H_{19}O_4^-$)] and **115** [m/z 229.1435 ($C_{12}H_{21}O_4^-$)] were observed in cluster I



and showed a mass difference of 14 amu due to extra CH_2 in **115** and were identified as undecanedioic acid and dodecanedioic acids, respectively.

A total of eighteen lipids were examined in the *K. elegans* extracts, which could be differentiated into two classes (*i.e.*, phospholipids and glycolipids). Among phospholipids, metabolites ascribable to phosphoinositols (PI), phosphoethanolamines (PE), phosphocholines (PC), and phosphatidic acids (PA) were tentatively identified. In particular, peak **119** [m/z 595.2859 ($\text{C}_{27}\text{H}_{48}\text{O}_{12}\text{P}^-$)], an example of PI, exhibited diagnostic fragment ions at m/z 315 and 241, due to dehydrated glycerophosphoinositol ($\text{C}_9\text{H}_{16}\text{O}_{10}\text{P}^-$) and inositol-phosphate ($\text{C}_6\text{H}_{10}\text{O}_8\text{P}^-$) ions, respectively. The ions at m/z 415 and 279 are related to the fatty acid-glycerophosphate ($\text{C}_{21}\text{H}_{36}\text{O}_6\text{P}^-$) and the 18:2 fatty acid carboxylate anion ($\text{C}_{18}\text{H}_{31}\text{O}_2^-$), respectively. However, the appearance of daughter ions at m/z 259, 153 and 79 led to their characterization as inositol phosphate ($\text{C}_6\text{H}_{12}\text{O}_9\text{P}^-$), dehydrated glycerol phosphate ($\text{C}_3\text{H}_6\text{O}_5\text{P}^-$) and phosphate (PO_3^-) ions, respectively. Compound **119** was identified as octadecadienyl-*glycero*-phospho-myo-inositol (PI (18:2/0:0)). The analysis of peak **127** MS/MS spectrum [m/z 452.2760 ($\text{C}_{21}\text{H}_{43}\text{NO}_7\text{P}^-$)], as an example of PE, showed the characteristic ions of phospholipids (m/z 153 and 79) and a base peak at m/z 255 corresponding to the 16:0 fatty acid carboxylate anion ($\text{C}_{16}\text{H}_{31}\text{O}_2^-$). The ions at m/z 214 and 140 represented glycerophosphoethanolamine ($\text{C}_5\text{H}_{13}\text{NO}_6\text{P}^-$) and phosphoethanolamine ($\text{C}_2\text{H}_7\text{NO}_4\text{P}^-$), respectively. Therefore, it was identified as hexadecanoyl-*sn-glycero*-phosphoethanolamine (PE (16:0/0:0)). PA was putatively identified as compound **137** [m/z 669.4466, $\text{C}_{37}\text{H}_{66}\text{O}_8\text{P}^-$]. It contained the diagnostic ions of phospholipids at m/z 153, 79 and 97 (H_2PO_4^-). Its major ions were observed at m/z 277 and 255 corresponding to the 18:3 ($\text{C}_{18}\text{H}_{29}\text{O}_2^-$) and 16:0 fatty acid carboxylate anions, respectively. Compound **137** was assigned as octadecatrienoyl-hexadecanoyl-*glycero*-phosphate (PA (18:3/16:0)). Compound **129** [m/z 520.3391, $\text{C}_{26}\text{H}_{51}\text{NO}_7\text{P}^+$], as a representative of PC, revealed product ion peaks at m/z 258, 184 and 104, corresponding to glycerolphosphocholine [$\text{C}_8\text{H}_{20}\text{NO}_6\text{P} + \text{H}^+$], phosphocholine [$\text{C}_5\text{H}_{14}\text{NO}_4\text{P} + \text{H}^+$] and choline [$\text{C}_5\text{H}_{13}\text{NO} + \text{H}^+$] ions, respectively. In addition, a specific ion at m/z 337, corresponding to dehydrated glycerol conjugated with 18:2 fatty acid ($\text{C}_{21}\text{H}_{37}\text{O}_3^+$), was observed. Accordingly, compound **129** was identified as octadecadienyl-*sn-glycero*-phosphocholine (PC (18:2)). The MS^2 spectra of glycolipids showed the typical product ions at m/z 253 and 235 attributed to the glyceryl hexoside anion ($\text{C}_9\text{H}_{17}\text{O}_8^-$) followed by dehydration, respectively. Compound **124** contained one hexose unit and it was identified as MGMG in cluster E. Cluster F contained peaks **117**, **120**, **122** and **126**, which exhibited an extra hexose moiety, and they showed fragment ions at m/z 415 and 397, corresponding to the glyceryl di-hexoside ion ($\text{C}_{15}\text{H}_{27}\text{O}_{13}^-$) and successive loss of water molecules, respectively. All glycolipids showed sharp peaks due to the involved fatty acid.

3.1.4. Amino and organic acids. UHPLC-MS/MS spectral analysis revealed the presence of amino acids, all were examined in both samples of *K. elegans*. They included proline

betaine (**7**), betaine (**11**), isoleucine (**17**) and phenylalanine (**27**). Their fragmentation pattern depended mainly on decarboxylation followed by loss of nitrogen-containing groups. The identified amino acids appeared in cluster G'.

A total of four organic acids were detected. Quinic and shikimic acids appeared mainly as scattered nodes in the negative MN, while guanidinobutanoic and kynurenic acids were present in the same cluster of amino acids, due to their nitrogen containment. The MS/MS spectra displayed abundant ions due to the loss of H_2O , CO_2 , CO and CH_2 groups, in addition to loss of nitrogen groups in the case of nitrogen-containing organic acid. The assessment of organic acids was based on their accurate masses, MS/MS fragmentation behaviors, and previous studies.⁴¹⁻⁴³

3.1.5. Other metabolites. Dihydrochalcones are polyphenols that exhibit a diversity of bioactivities, such as anti-inflammatory, anti-infective, and anti-carcinogenic.⁴⁴ A total of three phloretin molecules were putatively determined as compounds **95** [m/z 275.0911 ($\text{C}_{15}\text{H}_{15}\text{O}_5^+$)], **96** [m/z 435.1275 ($\text{C}_{21}\text{H}_{23}\text{O}_{10}^-$)] and **100** [m/z 435.1272 ($\text{C}_{21}\text{H}_{23}\text{O}_{10}^-$)]. Compound **95** was described as phloretin aglycone, while compounds **96** and **100** showed the typical fragmentation pattern of O-hexoside as evident from the fragment ion [$\text{M} - 162$]⁻ at m/z 273 besides the same daughter ions. Accordingly, these compounds were considered as isomers and identified as phloretin hexosides. Furthermore, isomer **100** was detected in KEL only.

Hydroxycoumarins and isocoumarins are listed in Table 1 as peaks **59**, **83** (isomers of scopoletin) and **60** (brevifolin carboxylic acid). They showed the characteristic fragmentation patterns of their classes in agreement with reference data.⁴⁵ In addition, specific product ions of **59** and **83** were mainly due to dehydration, while **60** corresponded to decarboxylation and dehydration.

Regarding the four examined phenols, peaks **19** [m/z 127.0387 ($\text{C}_6\text{H}_7\text{O}_3^+$)] and **21** [m/z 125.0239 ($\text{C}_6\text{H}_5\text{O}_3^-$)] were identified as pyrogallol,⁴⁶ while peaks **61** and **72** were identified as trimethoxyphenol [m/z 185.0805 ($\text{C}_9\text{H}_{13}\text{O}_4^+$)] and vaniliane [m/z 153.0544 ($\text{C}_8\text{H}_9\text{O}_3^+$)], respectively. Compounds **61** and **72** showed fragment ions mainly due to the loss of methoxy and carbonyl groups. Finally, peak **45** was identified as hydroxyquinoline,⁴⁷ with [$\text{M} + \text{H}$]⁺ at m/z 146.0598.

3.2. Toxicity study

Screening of the toxic effect of increased oral doses of KEL and KEF revealed that they were non-toxic up to 2000 mg kg^{-1} .

3.3. Morris water maze test

During the 4-day memory acquisition trial, the latency to find the hidden platform profoundly declined in all mice treated with STZ, with a profound deterioration in their cognitive functions in the second, third, and fourth training days, respectively, as compared to the NC group. The effect of the treatment with leaf or fruit extracts quickly normalized the mice memory from the second day (Table 2 and Fig. 5).

Table 2 Morris water maze test

Day/latency time (s)	Normal control	Positive control	KEL	KEF
Day 1	17.5 ± 2.5	114.9 ± 5	85.2 ± 6.4	24.3 ± 2.1
Day 2	17 ± 1	100 ± 10	21.2 ± 3.2	16.1 ± 3.2
Day 3	11.1 ± 3.2	100 ± 7.2	10.5 ± 2.1	11.6 ± 1.5
Day 4	9 ± 1	98 ± 2.6	8.2 ± 1.5	6.5 ± 1.5

KEL, *Koelreuteria elegans* leaf methanol extract and KEF, *Koelreuteria elegans* fruit methanol extract.

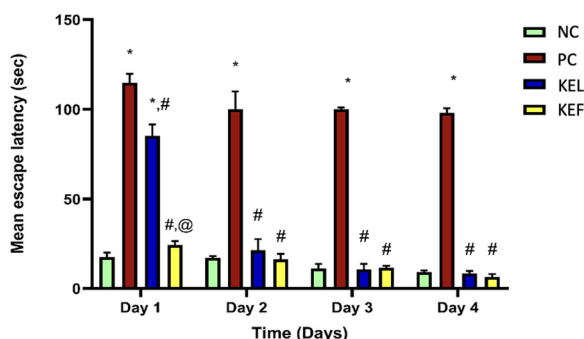


Fig. 5 Mean escape latency of KEL and KEF in memory function and spatial learning after a single injection of STZ (3 mg kg⁻¹, ICV) in the Morris water maze test. Statistical analysis was performed using one-way ANOVA followed by Tukey's multiple comparison test at $P < 0.05$. Data are expressed as mean ± SD ($n = 3$). * denotes a significant difference compared to NC, # denotes a significant difference compared to PC, and @ denotes a significant difference compared to the KEL-treated group. KEL, *Koelreuteria elegans* leaf extract; KEF, *Koelreuteria elegans* fruit extract; NC, negative control and PC, positive control.

3.4. Histopathological examination

Due to the involvement of the cerebral cortex in the memory function and being a primary target of Alzheimer's disease, it was chosen to assess the effect of different treatments. From the histopathology images it was apparent that the first group (NC) revealed a normal histological structure of the cerebral cortex. The untreated group (PC) showed various degenerated neurons in the cerebral cortex, which suggested a decline in the memory function. The group treated with the KEL showed a decline in the number of degenerated neurons with a moderate number of dark degenerated neurons in the cerebral cortex. Finally, the group treated with the KEF showed better modification of the degenerated neurons with only a few dark degenerated neurons in the cerebral cortex, suggesting a better outcome of treatment (Fig. 6).

3.5. The effect of *K. elegans* on TNF- α

The PC group showed a 4.6-fold increase in pro-inflammatory TNF- α ; this rise was controlled significantly by 38.5% upon the administration of KEL, with 70% decrease in the KEF treated group. Notably, the treatment with the fruit extract showed a 51% significant decline in the level of TNF- α compared to the group treated with the leaf extract (Table 3 and Fig. 7).

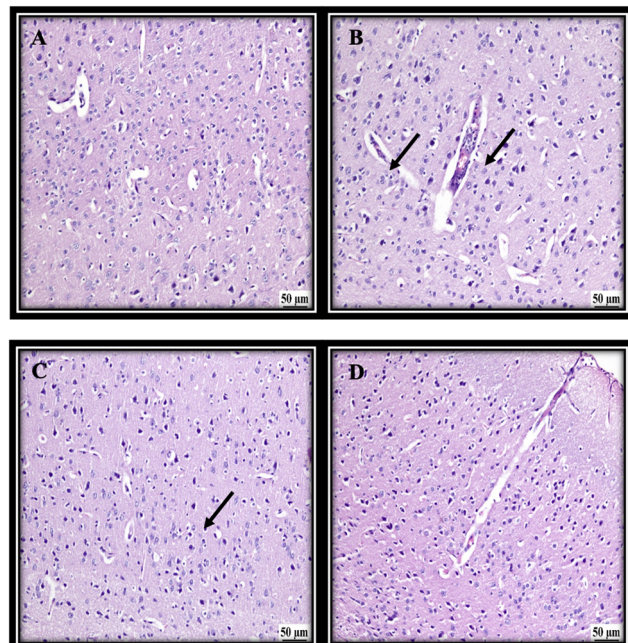


Fig. 6 Histopathological examination and microscopic examination of brain sections using hematoxylin & eosin staining for (A) normal control, (B) untreated group (positive control), showing a variable number of degenerated neurons in the cerebral cortex (arrows), (C) group treated with the *Koelreuteria elegans* leaf extract (KEL), showing a moderate number of dark degenerated neurons in the cerebral cortex, and (D) group treated with the *Koelreuteria elegans* fruit extract (KEF), showing a few degenerated neurons in the cerebral cortex.

3.6. The effect of *K. elegans* on NF- κ B

The transcription factor NF- κ B was increased by 82% in the PC group. The administration of KEL significantly controlled the level of NF- κ B, with 41% decline in its level. The KEF treated group exhibited 68.5% decline in the tissue NF- κ B level (Table 3 and Fig. 7).

3.7. The effect of *K. elegans* on IL-1 β

The increase in the IL-1 β level of the PC group (83.3%) was controlled significantly by the administration of KEL and KEF, with 37% and 69.8% decline in its level in the tissues, respectively (Table 3 and Fig. 7).

4. Discussion

Previous phytochemical studies of *K. elegans* led to the detection of phenolic compounds, flavonoids, lignans, sterols, tocopherols and triterpenes.^{11,14–21} Despite its potential as a producer of bioactive natural compounds, no studies are available on the anti-AD activity of *K. elegans*. The only study that discussed the anti-AD potential was conducted on *Koelreuteria paniculata*,¹ with the isolation and elucidation of five barrigenol-type triterpenoid compounds from the seeds of *K. paniculata*. These compounds were evaluated for their anti-AD activity in okadaic acid (OA)-induced learning and memory



Table 3 The influence of *K. elegans* leaf and fruit methanol extracts on the TNF- α /NF-KB/IL-1 β trajectory

Parameter/group	Normal control	Positive control	KEL	KEF
TNF- α	3.73 \pm 0.41	21 \pm 1	12.9 \pm 1.5	6.3 \pm 0.5
NF-KB	0.62 \pm 0.03	3.5 \pm 0.6	2.07 \pm 0.24	1.1 \pm 0.02
IL-1 β	4.03 \pm 0.3	24.2 \pm 0.85	15.3 \pm 0.95	7.3 \pm 0.33

TNF- α , tumor necrosis factor alpha; NF- κ B, nuclear factor kappa B; IL-1 β , interleukin-1 beta; KEL, *Koelreuteria elegans* leaf methanol extract; and KEF, *Koelreuteria elegans* fruit methanol extract.

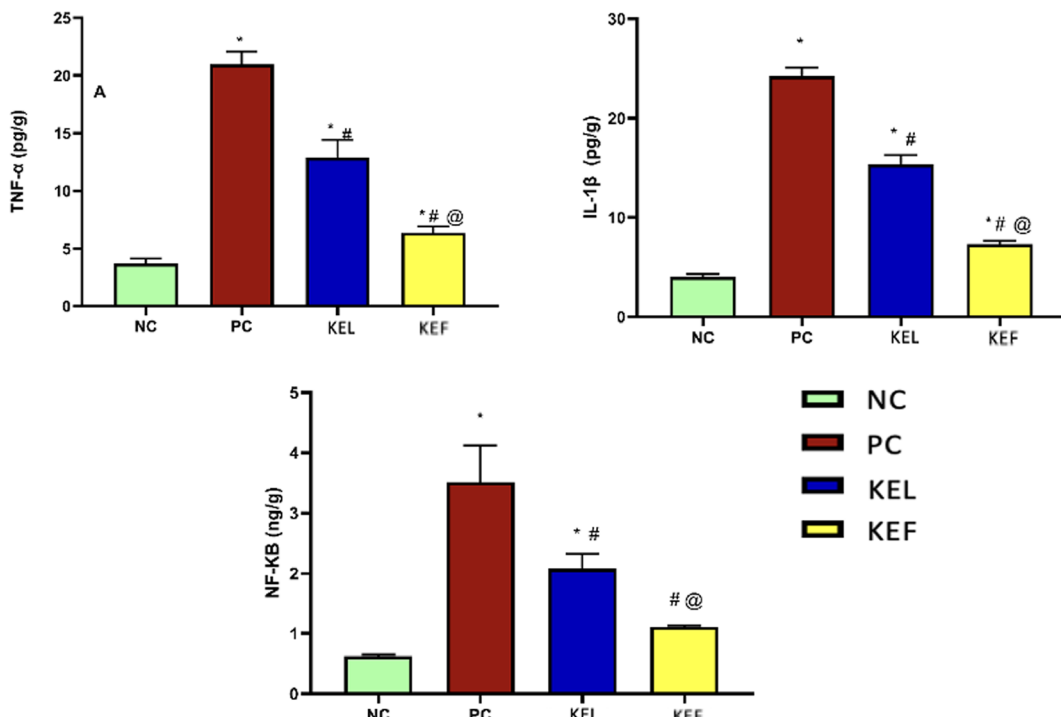


Fig. 7 The effect of the *K. elegans* extracts on the TNF- α /NF-KB/IL-1 β trajectory. KEL, *Koelreuteria elegans* leaf methanol extract; KEF, *Koelreuteria elegans* fruit methanol extract; NC, negative control; PC, positive control; TNF- α , tumor necrosis factor alpha; NF-KB, nuclear factor kappa B; and IL-1 β , interleukin-1 beta.

impaired mice. The results revealed that two of these metabolites could improve the learning and memory deficits induced by OA, along with the attenuation of the provoked tau hyperphosphorylation by regulating the levels of GSK-3 β and PP2A.¹ Our study identified secondary metabolites, such as phenolics, flavonoids and fatty acids. Phenolic acids have been demonstrated to attenuate the aggregation of proteins contributing to the pathogenesis of various neurodegenerative disorders characterized by cognitive deterioration, including Alzheimer's disease.^{48,49} Gallic, protocatechuic, ellagic and syringic acids detected in KEL and KEF have been previously evaluated for their potential to protect neurons from A β -induced neurotoxicity. They showed improvement of memory deficits and synaptic dysfunction by suppressing the release of the pro-inflammatory cytokines: TNF- α , NF- κ B, and IL-1 β .⁴⁸ Several studies evaluated the biological activities of flavonoids as neuronal antioxidants, exhibiting anti-amyloidogenic and anti-inflammatory potential and neuroprotection and improving cognition.⁵⁰⁻⁵⁵ *K. elegans* leaves and fruits are rich in

flavonoids, which have potential against AD by regulating several important physiological responses. Quercetin, catechin-3-gallate, apigenin, apigenin hexoside, kaempferol and luteolin are detected in KEL and KEF. They have been perceived in several reports as anti-neuroinflammatory by blocking the release of cytokines (TNF- α and IL-1 β), inhibiting NF- κ B expression, and reducing intracellular A β and the hyperphosphorylation of tau.⁵⁰⁻⁵³ The results of the study displayed that the fruit extract of *K. elegans* has a more potent anti-inflammatory effect than the leaf extract in a mice model of AD. The fruit extract reduced TNF- α , NF- κ B, and IL-1 β levels more than the leaf extract, which are all markers of inflammation and neurodegeneration in AD. This is consistent with some recent studies revealing that natural plant extracts can have beneficial effects on AD by modulating the immune system and clearing amyloid- β plaques.⁵⁶ The PC group, which represents an Alzheimer's disease model, showed sky-rocketed pro-inflammatory cytokine TNF- α levels. This is consistent with the well-documented involvement of TNF- α in neuroinflammation



and its association with Alzheimer's disease. Elevated TNF- α levels are often observed in the brains of AD patients and are thought to contribute to neuroinflammatory processes.⁴ Oxidative stress is known to play a significant role in the pathogenesis of neurodegenerative diseases, including Alzheimer's disease.

The capability of antioxidant drugs to shield neurons from amyloid-induced neurodegeneration is based on their ability to counteract oxidative stress and its detrimental effects on neuronal health.⁵⁷ In light of this, El Naggar *et al.* reported that *K. elegans* had a hepatoprotective effect due to its ability to increase the enzymatic levels of superoxide dismutase and glutathione, indicative of its antioxidant properties. Building on this, it is reasonable to propose that *K. elegans* extracts can exhibit neuroprotective effects.¹⁵ Furthermore, Kumari *et al.* demonstrated the antioxidant activity of *K. elegans* leaf extract using the DPPH method, and Waleed *et al.* supported these findings by confirming the strong radical scavenging properties of *K. elegans*. These studies collectively suggest the potential neuroprotective effects of *K. elegans* through its antioxidant mechanisms.¹² In addition, research has shown that antioxidant treatment can attenuate neuronal loss, improve cognitive function, and reduce the accumulation of amyloid β plaques in the brain.⁵⁸ These findings provide additional support for the notion that KE extracts may hold promise in slowing down the neurodegeneration process.

The administration of the leaf extract of *K. elegans* resulted in the decline of the levels of TNF- α , while the fruit extract of *K. elegans* led to an even more substantial diminution. This suggested that both extracts have anti-inflammatory effects, with the fruit extract being more effective. Affecting TNF- α triggers a trajectory that activates NF- κ B in the brain tissues.⁵⁹ The PC group exhibited an amplification in the transcription factor NF- κ B. Treatment with the leaf extract of *K. elegans* resulted in a reduction in NF- κ B levels, while the fruit extract showed a more extensive effect. In light of the previous parameters, the untreated mice group showed an upsurge in the pro-inflammatory cytokine IL-1 β , which is another key player in neuroinflammation associated with Alzheimer's disease.^{7,8} The effect of the fruit extract was more pronounced than that of the leaf extract in decreasing IL-1 β . These results indicated that both extracts have anti-inflammatory effects, with the fruit extract showing stronger activity. In the context of Alzheimer's disease research, these findings are promising. Since the antioxidant activity of the *K. elegans* extract was previously discussed,¹² this study sheds light on the anti-inflammatory capabilities of the plant extract. Neuroinflammation is increasingly recognized as a contributing factor to the progression of AD.² Hence, reducing pro-inflammatory markers like TNF- α , NF- κ B, and IL-1 β could have therapeutic potential. Further research, including clinical trials, is needed to determine the efficacy and safety of these extracts in humans with Alzheimer's disease.

5. Conclusion

The current study provides the first comprehensive metabolite profiles of leaf and fruit extracts of *K. elegans* using UHPLC-MS

in both negative and positive modes assisted by MN. A total of 139 metabolites were tentatively detected after a detailed interpretation of the data using the CSI:FingerID interface of Sirius 5.6.3.0 software, and the metabolite identification was further supported by MN exploration, together with the proposed GNPS spectral library search. The identified compounds belonged to various classes encompassing fifty-seven phenolic acids, thirty-seven flavonoids, four amino acids, four organic acids, four phenols, two hydroxycoumarins, one isocoumarin, three dihydrochalcones, and one hydroquinolone. Additionally, twenty-six lipids of different classes were characterized, including eight fatty acids, two phosphoinositols, three phosphoethanolamines, three phosphocholines, five glycolipids and five phosphatidic acids. The analysis of the data showed the compositional similarities and differences in the metabolites among the leaf and fruit extracts. Remarkably, KEL could ameliorate the learning and memory deficits induced by STZ in behavioral experiments, besides improving the histopathological profile of the cerebral cortex of the injured mice, while KEF led to an even more potent effect. Based on the *in vivo* experiments, the fruit extract reduced TNF- α , NF- κ B, and IL-1 β levels more than the leaf extract, which are all markers of inflammation and neurodegeneration in AD. Altogether, these findings provide support for further research with the raw leaf and fruit extracts or after fractionation and purification of specific compounds. More detailed and conclusive *in vivo* and clinical studies are highly recommended to exploit the potential of *K. elegans* in treating patients with Alzheimer's disease.

Abbreviations

AD	Alzheimer's disease
A β	Amyloid beta
CID	Collision induced dissociation
DAD	Diode-array detection
DDH	Dihydrodiol dehydrogenase
DGMG	Digalactosylmonoacylglycerol
ESI	Electrospray ionization
FBMN	Feature-based molecular network
GNPS	Global natural product social molecular networking
HRMS	High resolution mass spectrometry
ICV	Intracerebroventricular injection
IL-1 β	Interleukin-1 beta
IP	Intraperitoneal
KEF	<i>Koelreuteria elegans</i> fruit methanol extract
KEL	<i>Koelreuteria elegans</i> leaf methanol extract
MEL	Mean escape latency
MGMG	Monogalactosylmonoacylglycerol
MN	Molecular network
MWM	Morris water maze
NC	Normal control
NF- κ B	Nuclear factor kappa B
OECD	Organization for economic development
PA	Phosphatidic acid



PC	Positive control
PC	Phosphocholine
PE	Phosphoethanolamine
PI	Phosphoinositol
PTK	Protein-tyrosine kinase
ROS	Reactive oxygen species
STZ	Streptozotocin
TNF- α	Tumor necrosis factor alpha
UHPLC	Ultra high performance liquid chromatography

Conflicts of interest

There are no conflicts to declare.

References

- 1 X. Lu, L. Sun, Y. Zhang and W. Li, *J. Funct. Foods*, 2019, **61**, 103459.
- 2 M. Culjak, M. N. Perkovic, S. Uzun, D. S. Strac, G. N. Erjavec, M. B. Leko, G. Simic, L. Tudor, M. Konjevod, O. Kozumplik, N. Mimica and N. Pivac, *Curr. Alzheimer Res.*, 2020, **17**, 972–984.
- 3 F. Brosseron, M. Krauthausen, M. Kummer and M. T. Heneka, *Mol. Neurobiol.*, 2014, **50**, 534–544.
- 4 M. V. Lourenco, J. R. Clarke, R. L. Fozza, T. R. Bomfim, L. Forny-Germano, A. F. Batista, L. B. Sathler, J. Brito-Moreira, O. B. Amaral, C. A. Silva, L. Freitas-Correia, S. Espírito-Santo, P. Campello-Costa, J. C. Houzel, W. L. Klein, C. Holscher, J. B. Carvalheira, A. M. Silva, L. A. Velloso, D. P. Munoz, S. T. Ferreira and F. G. De Felice, *Cell Metab.*, 2013, **18**, 831–843.
- 5 E. Sun, A. Motolani, L. Campos and T. Lu, *Int. J. Mol. Sci.*, 2022, **23**.
- 6 Y. Tang, D. Zhang, X. Gong and J. Zheng, *Adv. Funct. Mater.*, 2022, **32**, 2208022.
- 7 D. Di Bona, A. Plaia, S. Vasto, L. Cavallone, F. Lescai, C. Franceschi, F. Licastro, G. Colonna-Romano, D. Lio, G. Candore and C. Caruso, *Brain Res. Rev.*, 2008, **59**, 155–163.
- 8 L. Xie, Y. Lai, F. Lei, S. Liu, R. Liu and T. Wang, *Mol. Med. Rep.*, 2015, **11**, 3219–3228.
- 9 F. Meyer, *J. Arnold Arbor.*, 1976, **57**, 129–166.
- 10 *Chinese medicinal plants*, ed. Y. C. Jeng, Publisher's Reader's Digest Association Far East Ltd., Hong Kong, 1994, vol. 207.
- 11 C. C. Wu, K. F. Huang, T. Y. Yang, Y. L. Li, C. L. Wen, S. L. Hsu and T. H. Chen, *PLoS One*, 2015, **10**, e0132052.
- 12 P. Kumari, S. Nehra and M. Deen, *J. Pharmacogn. Phytochem.*, 2019, **8**, 1724–1728.
- 13 W.-C. Tsai, H.-C. Chang, H.-Y. Yin, M.-C. Huang, D. C. Agrawal and H.-W. Wen, *Electron. J. Biotechnol.*, 2020, **47**, 89–99.
- 14 F. Abo-Elghiet, M. Ibrahim and A. A. Sleem, *Al-Azhar J. Pharm. Sci.*, 2021, **1**, 23–29.
- 15 D. El Naggar, *Al-Azhar J. Pharm. Sci.*, 2022, **65**, 16–39.
- 16 M. Abou-Shoer, G. E. Ma, X. H. Li, N. M. Koonchanok, R. L. Geahlen and C. J. Chang, *J. Nat. Prod.*, 1993, **56**, 967–969.
- 17 Y. N. Song, H. L. Zhang, C. J. Chang and D. M. Bollag, *J. Nat. Prod.*, 1994, **57**, 1670–1674.
- 18 T. H. Lee, Y. H. Chiang, C. H. Chen, P. Y. Chen and C. K. Lee, *J. Nat. Med.*, 2009, **63**, 209–214.
- 19 C. H. Chen, P. Y. Chen, K. C. Wang and C. K. Lee, *J. Chin. Chem. Soc.*, 2010, **57**, 404–410.
- 20 Y. Y. Chiang, S. L. Wang, C. L. Yang, H. Y. Yang, H. C. Yang, J. N. Sudhakar, C. K. Lee, H. W. Huang, C. M. Chen, S. H. Chiou, S. F. Chiang, H. Y. Fang, C. Y. Chen, S. H. Shieh and K. C. Chow, *Int. J. Mol. Med.*, 2013, **32**, 577–584.
- 21 C. Y. Lin, P. N. Chen, Y. S. Hsieh and S. C. Chu, *Food Chem.*, 2014, **146**, 299–307.
- 22 C. Y. Lin, P. N. Chen, L. S. Hsu, D. Y. Kuo, S. C. Chu and Y. S. Hsieh, *Mol. Med. Rep.*, 2014, **10**, 3334–3342.
- 23 M. H. Lee, C. B. Jiang, S. H. Juan, R. D. Lin and W. C. Hou, *Fitoterapia*, 2006, **77**, 109–115.
- 24 C. H. Chen, H. C. Chan, Y. T. Chu, H. Y. Ho, P. Y. Chen, T. H. Lee and C. K. Lee, *Molecules*, 2009, **14**, 2947–2958.
- 25 M. C. Chambers, B. Maclean, R. Burke, D. Amodei, D. L. Ruderman, S. Neumann, L. Gatto, B. Fischer, B. Pratt, J. Egertson, K. Hoff, D. Kessner, N. Tasman, N. Shulman, B. Frewen, T. A. Baker, M. Y. Brusniak, C. Paulse, D. Creasy, L. Flashner, K. Kani, C. Moulding, S. L. Seymour, L. M. Nuwaysir, B. Lefebvre, F. Kuhlmann, J. Roark, P. Rainer, S. Detlev, T. Hemenway, A. Huhmer, J. Langridge, B. Connolly, T. Chadick, K. Holly, J. Eckels, E. W. Deutsch, R. L. Moritz, J. E. Katz, D. B. Agus, M. MacCoss, D. L. Tabb and P. Mallick, *Nat. Biotechnol.*, 2012, **30**, 918–920.
- 26 C. J. Ugwah-Oguejiofor, C. O. Okoli, M. O. Ugwah, M. L. Umaru, C. S. Ogbulie, H. E. Mshelia, M. Umar and A. A. Njan, *Helijon*, 2019, **5**, e01179.
- 27 OECD, Test No. 425: Acute Oral Toxicity: Up-and-Down Procedure, 2022.
- 28 M. A. Pelleymounter, M. Joppa, M. Carmouche, M. J. Cullen, B. Brown, B. Murphy, D. E. Grigoriadis, N. Ling and A. C. Foster, *J. Pharmacol. Exp. Ther.*, 2000, **293**, 799–806.
- 29 M. A. Pelleymounter, M. Joppa, N. Ling and A. C. Foster, *J. Pharmacol. Exp. Ther.*, 2002, **302**, 145–152.
- 30 G. Warnock, 2007.
- 31 M. E. Sorial and N. El Sayed, *Naunyn Schmiedebergs Arch. Pharmacol.*, 2017, **390**, 581–593.
- 32 B. Singh, B. Sharma, A. S. Jaggi and N. Singh, *J. Renin Angiotensin Aldosterone Syst.*, 2013, **14**, 124–136.
- 33 T. M. M. Jouaneh, N. Motta, C. Wu, C. Coffey, C. W. Via, R. D. Kirk and M. J. Bertin, *Fitoterapia*, 2022, **159**, 105200.
- 34 N. Kumar and N. Goel, *Biotechnol. Rep.*, 2019, **24**, e00370.
- 35 W. Xu, M. Huang, H. Li, X. Chen, Y. Zhang, J. Liu, W. Xu, K. Chu and L. Chen, *J. Chromatogr. B: Anal. Technol. Biomed. Life Sci.*, 2015, **986–987**, 69–84.
- 36 M. d F. R. de Lima, L. A. Cavalcante, E. C. T. de Araújo Costa, B. O. de Veras, M. V. da Silva, L. N. Cavalcanti and R. M. Araújo, *Phytochem. Lett.*, 2021, **41**, 186–192.



37 A. N. Panche, A. D. Diwan and S. R. Chandra, *J. Nutr. Sci.*, 2016, **5**, e47.

38 A. Singh, S. Kumar and B. Kumar, *Nat. Prod. Commun.*, 2018, **13**(5), DOI: [10.1177/1934578X1801300511](https://doi.org/10.1177/1934578X1801300511).

39 R. M. Ibrahim, G. F. Elmasry, R. H. Refaey and R. A. El Shiekh, *ACS omega*, 2022, **7**, 17339–17357.

40 J. T. Pierson, G. R. Monteith, S. J. Roberts-Thomson, R. G. Dietzgen, M. J. Gidley and P. N. Shaw, *Food Chem.*, 2014, **149**, 253–263.

41 T. Guo, C. Tang, H. Song, Y. Dong and Q. Ma, *Food Chem.*, 2021, **353**, 129446.

42 S. Uysal, G. Zengin, K. I. Sinan, G. Ak, R. Ceylan, M. F. Mahomoodally, A. Uysal, N. B. Sadeer, J. Jekő, Z. Cziáky, M. J. Rodrigues, E. Yıldıztugay, F. Elbasan and L. Custodio, *RSC Adv.*, 2021, **11**, 5295–5310.

43 L. Chen, Z. Dai, C. Ge, D. Huang, X. Zhou, K. Pan, W. Xu, J. Fu and J. L. Du, *J. Chromatogr. B: Anal. Technol. Biomed. Life Sci.*, 2022, **1203**, 123260.

44 A. R. Jesus, A. P. Marques and A. P. Rauter, *Pure Appl. Chem.*, 2016, **88**, 349–361.

45 L. Cissé, A. Tine, L. Kaboré and A. Saba, *Spectrosc. Lett.*, 2009, **42**, 95–99.

46 I. E. Sallam, U. Rolle-Kampczyk, S. S. Schäpe, S. S. Zaghloul, R. S. El-Dine, P. Shao, M. V. Bergen and M. A. Farag, *Molecules*, 2022, **27**.

47 A. Ermakov, V. Voronin, A. Sorokin, N. Épshtain, I. Muravskaya, V. Chistyakov and A. Zuev, *Chem. Heterocycl. Compd.*, 1984, **20**, 637–642.

48 G. Caruso, J. Godos, A. Privitera, G. Lanza, S. Castellano, A. Chillemi, O. Bruni, R. Ferri, F. Caraci and G. Grossio, *Nutrients*, 2022, **14**.

49 Y. Tang, D. Zhang, X. Gong and J. Zheng, *Biophysical Chemistry*, 2022, **281**, 106735.

50 A. Calderaro, G. T. Patanè, E. Tellone, D. Barreca, S. Ficarra, F. Misiti and G. Laganà, *Int. J. Mol. Sci.*, 2022, **23**.

51 P. Bellavite, *Antioxidants*, 2023, **12**, 280.

52 R. A. Arias-Sánchez, L. Torner and B. Fenton Navarro, *Molecules*, 2023, **28**, 5415.

53 F. Hadrich, M. Chamkha and S. Sayadi, *Food Chem. Toxicol.*, 2022, **159**, 112752.

54 P. H. Nguyen, A. Ramamoorthy, B. R. Sahoo, J. Zheng, P. Faller, J. E. Straub, L. Dominguez, J.-E. Shea, N. V. Dokholyan and A. De Simone, *Chemical reviews*, 2021, **121**, 2545–2647.

55 Y. Tang, D. Zhang and J. Zheng, *ACS Chem. Neurosci.*, 2023, **14**, 3143–3155.

56 A. Halle, V. Hornung, G. C. Petzold, C. R. Stewart, B. G. Monks, T. Reinheckel, K. A. Fitzgerald, E. Latz, K. J. Moore and D. T. Golenbock, *Nat. Immunol.*, 2008, **9**, 857–865.

57 R. Dhapola, S. K. Beura, P. Sharma, S. K. Singh and D. HariKrishnaReddy, *Mol. Biol. Rep.*, 2024, **51**, 48.

58 S. Dubey and E. Singh, *Inflammopharmacology*, 2023, **31**, 717–730.

59 B. Kaltschmidt and C. Kaltschmidt, *Cold Spring Harb. Perspect. Biol.*, 2009, **1**, a001271.

